J|A|C|S
ARTICLES
Published on Web 02/10/2004

Utilization of Hydrogen Bonds To Stabilize M−O(H) Units: Synthesis and Properties of Monomeric Iron and Manganese Complexes with Terminal Oxo and Hydroxo Ligands

Cora E. MacBeth,[†] Rajeev Gupta,[†] Katie R. Mitchell-Koch,[†] Victor G. Young, Jr.,[‡] Gerald H. Lushington,[†] Ward H. Thompson,[†] Michael P. Hendrich,[§] and A. S. Borovik*[,†]

Contribution from the Department of Chemistry, University of Kansas, Lawrence, Kansas 66045, Department of Chemistry, University of Minnesota, Minneapolis, Minnesota 55455, and Department of Chemistry, Carnegie Mellon University, Pittsburgh, Pennsylvania 15213

Received August 28, 2003; E-mail: aborovik@ku.edu

Abstract: Non-heme iron and manganese species with terminal oxo ligands are proposed to be key intermediates in a variety of biological and synthetic systems; however, the stabilization of these types of complexes has proven difficult because of the tendency to form oxo-bridged complexes. Described herein are the design, isolation, and properties for a series of mononuclear Fe^{III} and Mn^{III} complexes with terminal oxo or hydroxo ligands. Isolation of the complexes was facilitated by the tripodal ligand tris[(*N′-tert*-butylureaylato)-*N*-ethyl]aminato ($[H_3\mathbf{1}]^{3-}$), which creates a protective hydrogen bond cavity around the M^{III}−O(H) units (M^{III} = Fe and Mn). The M^{III}−O(H) complexes are prepared by the activation of dioxygen and deprotonation of water. In addition, the M^{III}−O(H) complexes can be synthesized using oxygen atom transfer reagents such as *N*-oxides and hydroxylamines. The $[Fe^{III}H_3\mathbf{1}(O)]^{2-}$ complex also can be made using sulfoxides. These findings support the proposal of a high valent M^{IV}−oxo species as an intermediate during dioxygen cleavage. Isotopic labeling studies show that oxo ligands in the $[M^{III}H_3\mathbf{1}(O)]^{2-}$ complexes come directly from the cleavage of dioxygen: for $[Fe^{III}H_3\mathbf{1}(O)]^{2-}$ the $\nu(Fe-^{16}O) = 671\ cm^{-1}$, which shifts 26 cm^{-1} in $[Fe^{III}H_3\mathbf{1}(^{18}O)]^{2-}$ ($\nu(Fe-^{18}O) = 645\ cm^{-1}$); a $\nu(Mn-^{16}O) = 700\ cm^{-1}$ was observed for $[Mn^{III}H_3\mathbf{1}(^{16}O)]^{2-}$, which shifts to 672 cm^{-1} in the $Mn-^{18}O$ isotopomer. X-ray diffraction studies show that the Fe−O distance is 1.813(3) Å in $[Fe^{III}H_3\mathbf{1}(O)]^{2-}$, while a longer bond is found in $[Fe^{III}H_3\mathbf{1}(OH)]^{-}$ (Fe−O at 1.926(2) Å); a similar trend was found for the Mn^{III}−O(H) complexes, where a Mn−O distance of 1.771(5) Å is observed for $[Mn^{III}H_3\mathbf{1}(O)]^{2-}$ and 1.873(2) Å for $[Mn^{III}H_3\mathbf{1}(OH)]^{-}$. Strong intramolecular hydrogen bonds between the urea NH groups of $[H_3\mathbf{1}]^{3-}$ and the oxo and oxygen of the hydroxo ligand are observed in all the complexes. These findings, along with density functional theory calculations, indicate that a single σ-bond exists between the M^{III} centers and the oxo ligands, and additional interactions to the oxo ligands arise from intramolecular H-bonds, which illustrates that noncovalent interactions may replace π-bonds in stabilizing oxometal complexes.

Numerous oxidation reactions utilize metal complexes with terminal oxo ligands.[1] Among the late 3d transition-metal ions, iron and manganese oxo species in particular are purported to catalyze the oxidation of organic and biochemical substrates.[2] In biochemical systems, Mn−O species are proposed as intermediates in the oxygen evolving complex of photosystem II,[3] peroxidases,[4] and catalases.[5] Additionally, the catalytic cycles of many heme and non-heme iron enzymes involve species containing Fe−O units.[2,6] The metal centers in these species are postulated to have oxidation levels of greater than or equal to 4+; these assignments are made from low-temperature spectroscopic measurements[7] or mechanistic investigations.[8] Room-temperature isolation of monomeric Mn^{V}═O complexes has been achieved using tetraanionic chelating ligands.[9] Moreover, the structure of a non-heme Fe^{IV}═O

† University of Kansas.
‡ University of Minnesota.
§ Carnegie Mellon University.

(1) General references: (a) Sheldon, R. A.; Kochi, J. *Metal-Catalyzed Oxidations of Organic Compounds*; Academic: New York, 1981. (b) Holm, R. H. *Chem. Rev.* **1987**, *87*, 1401−1449. (c) Nugent, W. A.; Mayer, J. M. *Metal−Ligand Multiple Bonds*; Wiley-Interscience: New York, 1988. (d) Holm, R. H.; Donahue, J. P. *Polyhedron* **1993**, *12*, 571−589. (e) Abu-Omar, M. M. *Chem. Commun.* **2003**, 2102−2111.

(2) (a) *Biomimetic Oxidations Catalyzed by Transition Metal Complexes*; Meunier, B., Ed.; Imperial College Press: London, 2000. (b) Costas, M.; Chen, K.; Que, L., Jr. *Coord. Chem. Rev.* **2000**, *200*−*202*, 517−544. (c) Que, L., Jr.; Ho, R. Y. N. *Chem. Rev.* **1996**, *96*, 2607−2624. (d) Fontecave, M.; Ménage, S.; Duboc-Toia, C. *Coord. Chem. Rev.* **1998**, *178*−*180*, 1555−1572. (e) Groves, J. T.; Han, Y.-Z. In *Cytochrome P-450. Structure, Mechanism and Biochemistry*; Ortiz de Montellano, R. R., Ed.; Plenum Press: New York, 1995; pp 3−48. (f) Srinivasan, K.; Michaud, P.; Kochi, J. K. *J. Am. Chem. Soc.* **1986**, *108*, 2309−2390. (g) Zhang, W.; Loebach, J. L.; Wilson, S. R.; Jacobsen, R. N. *J. Am. Chem. Soc.* **1990**, *112*, 2801−2803. (h) Paluki, M.; Finney, N. S.; Pospisil, P. J.; Güler, M. L.; Ishida, T.; Jacobsen, E. N. *J. Am. Chem. Soc.* **1998**, *120*, 948−954. (i) *Metalloporphyrins in Catalytic Oxidations*; Sheldon, R. A., Ed.; M. Dekker: New York, 1994. (j) Nam, W.; Valentine, J. S. *J. Am. Chem. Soc.* **1993**, *115*, 1772−1778. (k) Groves, J. T.; Lee, J.; Marla, S. S. *J. Am. Chem. Soc.* **1997**, *119*, 6269−6273. (l) Jin, N.; Groves, J. T. *J. Am. Chem. Soc.* **1999**, *121*, 2923−2924.

10.1021/ja0305151 CCC: $27.50

complex has been reported recently that is stable at temperatures less than −20 °C.[10] The source of the oxo ligands in these manganese and iron−oxo complexes is derived from reagents other than dioxygen, such as peroxides or iodosylbenzene.[11]

Lower valent iron and manganese complexes (≤3+) with oxo ligands are dominated by species having $M^{III}-(\mu\text{-O})_n-M^{III}$ motifs (M^{III} = Fe, Mn; n = 1−3).[5a,12] Complexes of these metal ions containing terminal oxo ligands are rare: prior to our work, the polymeric $MeMn^{III}O\cdots Li$ species was the only structurally characterized system.[13] The paucity of stable Fe^{III}−oxo and Mn^{III}−oxo complexes reflects the widely held view that multiple bonds between the metal center and the terminal oxo ligand are required for isolation.[1] Multiple metal−oxo bonds often require vacant or half-filled π-accepting orbitals on the metal ion, which most often occurs for metal centers with oxidation states greater than 4+ and no more than four d electrons.[14]

A growing body of evidence suggests that other interactions can influence the stability of terminal oxo metal units. In particular, structure−function studies on metalloproteins indicate that intramolecular hydrogen bonds (H-bonds) can regulate the properties of the oxometal complexes. For instance, X-ray diffraction studies (2.2 Å resolution) on compound I of cytochrome *c* peroxidase show that H-bonds exist between an active-site arginine (Arg48) and the Fe^{IV}═O center.[15] Spectroscopic measurements on compound II of horseradish peroxidase[16] and theoretical studies of models for bleomycin[17] and methane monooxygenase[18] further suggest that activity is partially regulated by H-bonds to oxoiron units. These intramolecular interactions occur between the oxo ligand and an H-bond donor(s) positioned within the active site. The protein-induced microenvironment that surrounds the oxometal complex facilitates this type of multiple bond formation.

We are developing synthetic systems that utilize principles of metalloprotein architecture to study the role of H-bonds in dioxygen activation and stabilization of terminal M−oxo units.[19−21] Key components of our systems include multidentate ligands that bind metal ions and rigid organic frameworks that promote *intramolecular* H-bonds to M−O(H) units. The anionic forms of tris[(*N'*-*tert*-butylureayl)-*N*-ethyl]amine ([H_6**1**]) accomplish this by creating H-bond cavities around vacant coordination sites when coordinated to a metal ion. Deprotonation of the αNH groups yields the trianionic ligand, [H_3**1**]$^{3-}$, where metal ion binding is achieved through the three αN^- and one amine nitrogen sites. The remaining components of the urea groups serve as scaffolding for a cavity that disposes three H-bond donors proximal to a fifth ligand coordinated trans to the apical amine nitrogen. The rigidity of the urea groups combined with the formation of thermodynamically favored six-membered rings upon H-bond formation suggested to us that intramolecular interactions would be favored.

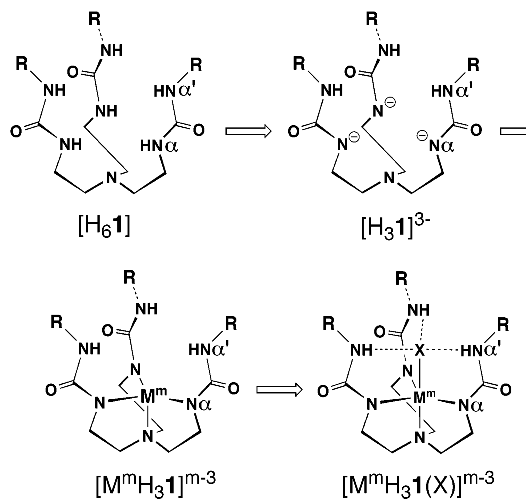

[H_6**1**] [H_3**1**]$^{3-}$ [M^mH_3**1**]$^{m-3}$ [M^mH_3**1**(X)]$^{m-3}$

(3) (a) Yachandra, V. K.; Sauer, K.; Klein, M. P. *Chem. Rev.* **1996**, *96*, 2927−2950. (b) Tommos, C.; Babcock, G. T. *Acc. Chem. Res.* **1998**, *31*, 18−25 and references therein. (c) Pecoraro, V. L.; Baldwin, M. J.; Caudle, M. T.; Hsieh, W.-Y.; Law, N. A. *Pure Appl. Chem.* **1998**, *70*, 925−929. (d) Tang, X.-S.; Ball, J. A.; Randall, D. W.; Force, D. A.; Diner, B. A.; Britt, R. D. *J. Am. Chem. Soc.* **1996**, *118*, 7638−7639. (e) Gilchrist, M. L., Jr.; Ball, J. A.; Randall, D. W.; Britt, R. D. *Proc. Natl. Acad. Sci. U.S.A.* **1995**, *92*, 9545−9549.

(4) Nicks, R. J.; Ray, G. B.; Fish, K. M.; Spiro, T. G.; Groves, J. T. *J. Am. Chem. Soc.* **1991**, *113*, 1838−1840.

(5) (a) Pecoraro, V. L.; Baldwin, M. J.; Gelasco, A. *Chem Rev.* **1994**, *94*, 807. (b) Dismukes, G. C. *Chem. Rev.* **1996**, *96*, 2909−2926.

(6) (a) Merkx, M.; Kopp, D. A.; Sazinsky, M. H.; Blazyk, J. L.; Müller, J.; Lippard, S. J. *Angew. Chem., Int. Ed.* **2001**, *40*, 2782−2807. (b) Que, L., Jr.; Tolman, W. B. *Angew. Chem., Int. Ed.* **2002**, *41*, 1114−1137.

(7) (a) Balch, A. L.; Chan, Y.-W.; Cheng, R.-J.; La Mar, G. N.; Latos-Grazynski, L.; Renner, M. W. *J. Am. Chem. Soc.* **1984**, *106*, 7779−7785. (b) Solomon, E. I.; Brunold, T. C.; Davis, M. I.; Kemsley, J. N.; Lee, S.-K.; Lennert, N.; Neese, F.; Skulan, A.; Yang, Y.-S.; Zhou, J. *Chem. Rev.* **2000**, *100*, 235−349 and references therein. (c) Grapperhaus, C. A.; Mienert, B.; Bill, E.; Weyhermüller, T.; Wieghardt, K. *Inorg. Chem.* **2000**, *39*, 5306−5317. (d) Lange, S. J.; Miyake, H.; Que, L., Jr. *J. Am. Chem. Soc.* **1999**, *121*, 6330−6331.

(8) (a) Groves, J. T.; der Puy; M. V. *J. Am. Chem. Soc.* **1974**, *96*, 5274−5275. (b) Mukerjee, S.; Stassinopoulos, A.; Caradonna, J. P. *J. Am. Chem. Soc.* **1997**, *119*, 8097−8098. (c) Stassinopoulos, A.; Mukerjee, S.; Caradonna, J. P. In *Reactivity Models for Dinuclear Iron Metalloenzymes: Oxygen Atom Transfer, Catalysis and Dioxygen Activation*; Stassinopoulos, A., Mukerjee, S., Caradonna, J. P., Eds.; American Chemical Society: Washington, DC, 1994; Vol. 246, pp 83−120. (d) Costas, M.; Tipton, A. K.; Chen, K.; Jo, D.-H.; Que, L., Jr. *J. Am. Chem. Soc.* **2001**, *123*, 6722−6723. (e) Chen, K.; Que, L., Jr. *J. Am. Chem. Soc.* **2001**, *123*, 6327−6337. (f) White, M. C.; Doyle, A. G.; Jacobsen, E. N. *J. Am. Chem. Soc*. **2001**, *123*, 7194−7195.

(9) (a) Collins, T. J.; Gordon-Wylie, S. W. *J. Am. Chem. Soc.* **1989**, *111*, 4511−4512. (b) Collins, T. J.; Powell, R. D.; Slebodnick, C.; Uffelman, E. S. *J. Am. Chem. Soc.* **1990**, *112*, 899−901. (c) Mandimutsira, B. S.; Ramdhanie, B.; Todd, R. C.; Wang, H.; Zareba, A. A.; Czernuszewicz, R. S.; Goldberg, D. P. *J. Am. Chem. Soc.* **2002**, *124*, 15170−15171.

(10) Rohde, J.-U.; In, J.-H.; Lim, M. H.; Brennessel, W. W.; Bukowski, M. R.; Stubna, A.; Münck, E.; Nam, W.; Que, L., Jr. *Science* **2003**, *299*, 1037−1039.

(11) Notable exception: MacDonnell, F. M.; Fackler, N. L. P.; Stern, C.; O'Halloran, T. V. *J. Am. Chem. Soc.* **1994**, *116*, 7431−7432.

(12) (a) Kurtz, D. M., Jr. *Chem. Rev.* **1990**, *90*, 585−606. (b) Feig, A. L.; Lippard, S. J. *Chem. Rev.* **1994**, *94*, 759−805. (c) Wieghardt, K. *Angew. Chem., Int. Ed. Engl.* **1989**, *28*, 1153.

(13) Morris, R. J.; Girolomi, G. S. *Polyhedron* **1988**, *7*, 2001−2008.

(14) For examples of d^4 and d^6 oxometal complexes, see: (a) Mayer, J. M.; Thorn, D. L.; Tulip, T. H. *J. Am. Chem. Soc.* **1985**, *107*, 7454−7462. (b) Wilkinson, G.; Hay-Motherwell, R.; Hussian-Bates, B.; Hursthouse, M. B. *Polyhedron* **1993**, *12*, 2009−2012. (c) Cheng, W.-C.; Yu, W.-Y.; Cheung, K.-K.; Che, C.-M. *J. Chem. Soc., Dalton Trans.* **1994**, 57−62. (d) Welch, T. W.; Ciftan, S. A.; White, P. S.; Thorp, H. H. *Inorg. Chem*. **1997**, *36*, 4812−4821. (e) Spaltenstein, E.; Conry, R. R.; Critchlow, S. C.; Mayer, J. M. *J. Am. Chem. Soc.* **1989**, *111*, 8741−8742.

(15) Fülöp, V.; Phizackerley, R. P.; Soltis, S. M.; Clifton, I. J.; Wakatuski, S.; Erman, J.; Hajdu, J.; Edwards, S. L. *Structure* **1994**, *2*, 201−208.

(16) Mukai, M.; Nagano, S.; Tanaka, M.; Ishimori, K.; Morishima, I.; Ogura, T.; Watanabe Y.; Kitagawa, T. *J. Am. Chem. Soc.* **1997**, *119*, 1758−1766.

(17) Wu, Y.-D.; Houk, K. S.; Valentine, J. S.; Nam, W. *Inorg. Chem*. **1992**, *31*, 718−720.

(18) (a) Dunietz, B. D.; Beachy, M. D.; Cao, Y.; Whittington, D. A.; Lippard, S. J.; Friesner, R. A. *J. Am. Chem. Soc.* **2000**, *122*, 2828−2839. (b) Gherman, B. F.; Dunietz, B. D.; Whittington, D. A.; Lippard, S. J.; Friesner, R. A. *J. Am. Chem. Soc.* **2001**, *123*, 3836−3837.

(19) (a) Hammes, B. S.; Young, V. G., Jr.; Borovik, A. S. *Angew. Chem., Int. Ed.* **1999**, *38*, 666−669. (b) Shirin, Z.; Hammes, B. S.; Young, V. G., Jr.; Borovik, A. S. *J. Am. Chem. Soc.* **2000**, *122*, 1836−1837. (c) MacBeth, C. E.; Golombek, A. P.; Young, V. G., Jr.; Yang, C.; Kuczera, K.; Hendrich, M. P.; Borovik, A. S. *Science* **2000**, *289*, 938−941. (d) MacBeth, C. E.; Hammes, B. S.; Young, V. G., Jr.; Borovik, A. S. *Inorg. Chem.* **2001**, *40*, 4733−4741. (e) Gupta, R.; MacBeth, C. E.; Young, V. G., Jr.; Borovik, A. S. *J. Am. Chem. Soc.* **2002**, *124*, 1136−1137.

(20) (a) MacBeth, C. E.; Larsen, P. L.; Sorrell, T. N.; Powell, D.; Borovik, A. S. *Inorg. Chim. Acta* **2002**, *341*, 77−84. (b) Larsen, P. L.; Parolin, T. J.; Powell, D. R.; Hendrich, M. H.; Borovik, A. S. *Angew. Chem., Int. Ed.* **2003**, *42*, 85−89.

Other synthetic complexes have been reported that contain H-bond donors positioned near metal ions.[22] These include iron porphyrin complexes for reversible O_2 binding,[23] the "hangman" iron porphyrins designed to model structural aspects of the active site in cytochrome P450,[24] and metal complexes of pyridine[25] and imidazole-based[26] tripodal ligands. Additional designs have complexes where these interactions aid in molecular recognition processes.[27]

Metal complexes of $[H_3\mathbf{1}]^{3-}$ differ from these previously reported systems by having a highly anionic primary coordination sphere contained within a relatively small H-bond cavity. These properties permit Fe^{II} and Mn^{II} complexes of $[H_3\mathbf{1}]^{3-}$ to activate dioxygen and produce monomeric $M^{III}-O(H)$ species. Furthermore, the constrained microenvironment around the $M-O(H)$ unit prevents formation of $M^{III}-(\mu\text{-}O)_n-M^{III}$ species, the common oxidation products from Fe^{II} and Mn^{II} mediated dioxygen activation (vide supra). Reported herein are the formation and properties of this new class of oxometal complexes. Our results demonstrate the utility of this design for isolating complexes with terminal oxo and hydroxo ligands, and that noncovalent interactions can be used in stabilizing $M^{III}-$oxo units.

Experimental Section

Preparative Methods and Syntheses. All reagents were purchased from commercial sources and used as received, unless otherwise noted. Anhydrous solvents were purchased from Aldrich. Dioxygen was dried on a Drierite gas purifier that was purchased from Fisher Scientific. The syntheses of all metal complexes were conducted in a Vacuum Atmosphere drybox under an argon atmosphere. Elemental analyses of all compounds were performed at Desert Analytics, Tucson, AZ. All samples were dried in vacuo before analysis. The presence of solvates was corroborated by FTIR and ^1H NMR spectroscopy. $H_6\mathbf{1}$ was synthesized using literature methods.[19b,c] The preparations of $K_2[Mn^{III}H_3\mathbf{1}(O)]$, $K[Mn^{III}H_3\mathbf{1}(OH)]$, and $K[Fe^{III}H_3\mathbf{1}(OH)]$ from water have been reported previously.[19d,e] All experimental procedures were repeated at least in duplicate, and yields are reported as average values.

Syntheses with Dioxygen. Potassium {Tris[(*N*′-*tert*-butylureaylato)-*N*-ethyl]aminato(oxo)ferrate(III)} ($K_2[Fe^{III}H_3\mathbf{1}(O)]$). $H_6\mathbf{1}$ (0.200 g, 0.451 mmol) was dissolved in ~10 mL dimethylacetamide (DMA) and treated with solid KH (0.072 g, 1.8 mmol) under an argon atmosphere. The mixture was stirred until hydrogen gas evolution ceased. This mixture was then treated with solid $Fe(OAc)_2$ (0.079 g, 0.45 mmol) and stirred for 10 min. Dry O_2 (5.5 mL, 0.23 mmol) was added to the reaction mixture through a gastight syringe, and immediately a deep orange solution resulted. The reaction mixture was stirred for 1 h and placed under reduced pressure for 5 min. The mixture was then filtered to remove 2 equiv of KOAc (0.080 g, 90%). The resulting orange filtrate was concentrated to dryness, and the crude compound was isolated after washing with diethyl ether. Diffusing diethyl ether vapors into a DMA solution of the crude salt afforded the recrystallized salt. Yield: 0.19 g (70%). Anal. Calcd (found) for $K_2[Fe^{III}H_3\mathbf{1}(O)]\cdot$DMA, $C_{25}H_{52}N_8O_5K_2Fe$: C, 44.24 (43.96); H, 7.72 (7.95); N, 16.50 (16.02). FTIR (Nujol, cm^{-1}): ν(NH) 3230, 3140 (urea, s); ν(CO) 1640, 590 (DMA, s), 1600, 1530 (urea, s); $\nu(Fe-^{16}O)$ 671, $\nu(Fe-^{18}O)$ 645. $\lambda_{max/nm}$ (DMA, ϵ, $M^{-1}\ cm^{-1}$): 291 (2900) and 392 (2100); $\lambda_{max/nm}$ (DMSO, ϵ, $M^{-1}\ cm^{-1}$): 395 (1940). EPR (DMA, 77 K): $g = 5.5$ and 1.98. μ_{eff} (solid, 298 K) = 5.93 μ_B.

Potassium {Tris[(*N*′-*tert*-butylureaylato)-*N*-ethyl]aminato(oxo)manganate(III)} ($K_2[Mn^{III}H_3\mathbf{1}(O)]$). $K_2[Mn^{III}H_3\mathbf{1}(O)]$ was prepared using the same procedure as for $K_2[Fe^{III}H_3\mathbf{1}(O)]$ with $H_6\mathbf{1}$ (0.200 g, 0.451 mmol), KH (0.072 g, 1.8 mmol), and $Mn(OAc)_2$ (0.078 g, 0.45 mmol). Crude compound was not isolated; the filtrate was layered with diethyl ether to obtain crystalline product as purplish-brown solid in 68% yield (0.18 g). Anal. Calcd (found) for $K_2[Mn^{III}H_3\mathbf{1}(O)]\cdot$2DMA, $C_{29}H_{60}N_9O_6K_2Mn$: C, 45.60 (45.43); H, 7.86 (8.06); N, 16.51 (16.26). FTIR (Nujol, cm^{-1}): ν(NH) 3242, 3153 (urea, s); ν(CO) 1639, 590 (DMA, s), 1598, 1520 (urea, s); $\nu(Mn-^{16}O)$ 700, $\nu(Mn-^{18}O)$ 672. $\lambda_{max/nm}$ (DMA, ϵ, $M^{-1}\ cm^{-1}$): 498 (410) and 715 (255); $\lambda_{max/nm}$ (DMSO, ϵ, $M^{-1}\ cm^{-1}$): 498 (490) and 725 (240). μ_{eff} (solid, 298 K) = 4.95 μ_B.

Potassium {Tris[(*N*′-*tert*-butylureaylato)-*N*-ethyl]aminato(hydroxo)ferrate(III)} ($K[Fe^{III}H_3\mathbf{1}(OH)]$). $H_6\mathbf{1}$ (0.200 g, 0.451 mmol) was dissolved in ~10 mL of DMA and treated with solid KH (0.054 g, 1.4 mmol) under an argon atmosphere. The mixture was stirred until H_2 evolution ceased. Solid $Fe(OAc)_2$ (0.079 g, 0.45 mmol) was added to the above mixture and stirred for additional 10 min. Dry O_2 (5.5 mL, 0.23 mmol) was injected into the reaction mixture through a gastight syringe, and immediately a deep red solution resulted. The reaction mixture was stirred for 1 h and then evacuated for 5 min. The mixture was filtered to remove 2 equiv (0.085 g, 96%) of KOAc. The resulting dark red filtrate was concentrated to dryness, and the crude compound was isolated after being washed with diethyl ether. This salt was recrystallized from MeCN after vapor diffusion of diethyl ether. A fine dark red microcrystalline solid was isolated, washed with diethyl ether, and dried under *vacuum* to yield 0.15 g (60%). Anal. Calcd (found) for $K[Fe^{III}H_3\mathbf{1}(OH)]\cdot$2DMA, $C_{29}H_{61}N_9O_6KFe$: C, 47.92 (47.89); H, 8.45 (8.02); N, 17.34 (17.78). FTIR (Nujol, cm^{-1}): $\nu(^{16}OH)$ 3630; $\nu(^{18}OH)$ 3621; ν(NH) 3270, 3180 (urea, s); ν(CO) 1590, 1540 (urea, s). $\lambda_{max/nm}$ (DMA, ϵ, $M^{-1}\ cm^{-1}$): 382 nm (4000); $\lambda_{max/nm}$ (DMSO, ϵ, $M^{-1}\ cm^{-1}$): 396 (3950). EPR (DMA, 77 K): $g = 8.9$, 5.3, 3.4, 1.3. μ_{eff} (solid, 297 K) = 5.99 μ_B.

(21) Zart, M. K.; Sorrell, T. N.; Powell, D.; Borovik, A. S. *J. Chem. Soc., Dalton Trans.* **2003**, 1986−1992.
(22) Representative examples: (a) Walters, M. A.; Dewan, J. C.; Min, C.; Pinto, S. *Inorg. Chem.* **1991**, *30*, 2656−2662. (b) Kitajima, N.; Komatsuzaki, H.; Hikichi, S.; Osawa, M.; Moro-oka, Y. *J. Am. Chem. Soc.* **1994**, *116*, 11596−11597. (c) Huang, J.; Ostrader, R. L.; Rheingold, A. L.; Walters, M. A. *Inorg. Chem.* **1995**, *34*, 1090−1093. (d) Millar, M.; Nguyen, D.; Voorhies, H.; Beatty, S.; Haff, J.; Dejean, F. *Abstracts of Papers*, 216th National Meeting of the American Chemical Society, Boston, MA, Aug 23−27, 1998; American Chemical Society: Washington, DC, 1998; INOR-351. (e) Peris, E.; Lee, J. C., Jr.; Rambo, J. R.; Eisenstein, O.; Crabtree, R. H. *J. Am. Chem. Soc.* **1995**, *117*, 3485−3491. (f) Lough, A. J.; Park, S.; Ramachandran, R.; Morris, R. H. *J. Am. Chem. Soc.* **1994**, *116*, 8356−8357. (g) Biradha, K.; Desiraju, G. R. *Organometallics* **1997**, *16*, 1846−1856. (h) Calhorda, M. J. *Chem. Commun.* **2000**, 801−809. (i) Quinn, R.; Mercer-Smith, J.; Burstyn, J. N.; Valentine, J. S. *J. Am. Chem. Soc.* **1984**, *106*, 4136−4139.
(23) (a) Momenteau, M.; Reed, C. A. *Chem. Rev.* **1994**, *94*, 659−698 and references therein. (b) Collman, J. P. *Acc. Chem. Res.* **1977**, *10*, 265−275. (c) Jameson, G. B.; Drago, R. S. *J. Am. Chem. Soc.* **1985**, *107*, 3017−3022. (d) Collman, J. P.; Zhang, X.; Wong, K.; Bauman, J. I. *J. Am. Chem. Soc.* **1994**, *116*, 6245−6251. (e) Wuenschell, G. E.; Tetreau, C.; Lavalette, D.; Reed, C. A. *J. Am. Chem. Soc.* **1992**, *114*, 3346−3355. (f) Chang, C. K.; Liang, Y.; Avilés, G.; Peng, S.-M. *J. Am. Chem. Soc.* **1995**, *117*, 4191−4192. (g) Collman, J. P.; Fu, L. *Acc. Chem. Res.* **1999**, *32*, 455−463.
(24) Yeh, C.-Y.; Chang, C. J.; Nocera, D. G. *J. Am. Chem. Soc.* **2001**, *123*, 1513−1514.
(25) (a) Harata, M.; Jitsukawa, K.; Masuda, H.; Einaga, H. *J. Am. Chem. Soc.* **1994**, *116*, 10817−10818. (b) Harata, M.; Jitsukawa, K.; Masuda, H.; Einaga, H. *Chem. Lett.* **1995**, 61−62. (c) Berreau, L. M.; Mahapatra, S.; Halfen, J. A.; Young, V. G., Jr.; Tolman, W. B. *Inorg. Chem.* **1996**, *35*, 6339−6342. (d) Wada, A.; Harata, M.; Hasegawa, K.; Jitsukawa, K.; Masuda, H.; Mukai, M.; Kitagawa, T.; Einaga, H. *Angew. Chem., Int. Ed.* **1998**, *37*, 798−799. (e) Ogo, S.; Yamahara, R.; Roach, M.; Suenobu, T.; Aki, M.; Ogura, T.; Kitagawa, T.; Masuda, H.; Fukuzumi, S.; Watanabe, Y. *Inorg. Chem.* **2002**, *41*, 5513−5520. (f) Berreau, L. M.; Allred, R. A.; Makowski-Grzyska, M. M.; Arif, A. M. *Chem. Commun.* **2000**, 1423−1424. (g) Berreau, L. M.; Makowska-Grzyska, M. M.; Arif, A. M. *Inorg. Chem.* **2001**, *40*, 2212−2213. (h) Garner, D. K.; Allred, R. A.; Tubbs, K. J.; Arif, A. M.; Berreau, L. M. *Inorg. Chem.* **2002**, *41*, 3533−3541. (i) Berreau, L. M.; Makowska-Grzyska, M. M.; Arif, A. M. *Inorg. Chem.* **2000**, *39*, 4390−4391. (j) Garner, D. K.; Fitch, S. B.; McAlexander, L. H.; Bezold, L. M.; Arif, A. M.; Berreau, L. M. *J. Am. Chem. Soc.* **2002**, *124*, 9970−9971.
(26) Cheruzel, L. E.; Wang, J.; Mashuta, M. S.; Buchanan, R. M. *Chem. Commun.* **2002**, 2166−2167.
(27) Selected examples: (a) Kickham, J. E.; Loeb, S. L.; Murphy, S. L. *J. Am. Chem. Soc.* **1993**, *115*, 7031−7032. (b) Rudkevich, D. M.; Verboom, W.; Brzozka, Z.; Palys, M. J.; Stauthamer, W. P. R. V.; Van Hummel, G. J.; Franken, S. M.; Harkema, S.; Engbersen, J. F. J.; Reinhoudt, D. N. *J. Am. Chem. Soc.* **1994**, *116*, 4341−4351. (c) Walton, P. H.; Raymond, K. N. *Inorg. Chim. Acta* **1995**, *240*, 593−601.

Potassium {Tris[(*N′*-*tert*-butylureaylato)-*N*-ethyl]aminato(hydroxo)-manganate(III)} (K[$Mn^{III}H_3$1(OH)]). K[$Mn^{III}H_3$**1**(OH)] was prepared following the procedure used for K[$Fe^{III}H_3$**1**(OH)] with H_6**1** (0.200 g, 0.451 mmol), KH (0.054 g, 1.4 mmol), and $Mn(OAc)_2$ (0.078 g, 0.45 mmol). K[$Mn^{III}H_3$**1**(OH)] was isolated as green solid in 52% recrystallized yield (0.13 g). Anal. Calcd (found) for K[$Mn^{III}H_3$**1**(OH)], $C_{21}H_{43}N_7O_4KMn$: C, 45.73 (45.49); H, 7.86 (7.82); N, 17.77 (17.88). FTIR (Nujol, cm^{-1}): $\nu(^{16}OH)$ 3614, $\nu(^{18}OH)$ 3603; ν(NH) 3265, 3178 (urea, s); ν(CO) 1603, 1527 (urea, s). $\lambda_{max/nm}$ (DMA, ϵ, M^{-1} cm^{-1}): 435 (280) and 724 (520); $\lambda_{max/nm}$ (DMSO, ϵ, M^{-1} cm^{-1}): 427 (390) and 710 (500). μ_{eff} (solid, 297 K) = 4.94 μ_B.

Synthesis with Water. K_2[$Fe^{III}H_3$1(O)]. H_6**1** (0.200 g, 0.450 mmol) was dissolved in ~10 mL of DMA and treated with solid KH (0.091 g, 2.3 mmol) under an argon atmosphere. The mixture was stirred until H_2 evolution ceased, after which solid $Fe(OAc)_2$ (0.079 g, 0.45 mmol) was added in one portion. After being stirred for 10 min, the mixture was filtered to remove KOAc (0.083 g, 93%), and water (8.1 μL, 0.45 mmol) was added via a gastight syringe. The reaction was stirred for an additional 10 min, and then [$FeCp_2$]BF_4 (0.124 g, 0.455 mmol) was added as a 1 mL DMA solution. The resulting deep orange solution was stirred for 1 h and filtered through a medium porous glass frit. The filtrate was concentrated under reduced pressure and washed three times with 5 mL of diethyl ether to remove ferrocene. Diffusing diethyl ether vapors into a DMA solution of the crude salt afforded 0.17 g (64%) of title salt. This sample had identical spectroscopic properties as the compound synthesized from dioxygen.

Syntheses with Amine-*N*-Oxides. Preparation of K_2[$Fe^{III}H_3$1(O)]. With Trimethylamine-*N*-oxide (Me_3NO): H_6**1** (0.180 g, 0.410 mmol) was treated with solid KH (0.065 g, 1.6 mmol) in ~10 mL of DMA under an argon atmosphere. The mixture was stirred until H_2 gas evolution ceased, followed by the addition of solid $Fe(OAc)_2$ (0.071 g, 0.41 mmol) in one portion. KOAc (0.077 g, 96%) was removed via filtration through a medium porous glass frit. The resulting pale yellow filtrate was treated with Me_3NO (0.034 g, 0.45 mmol) and stirred for 1 h. Volatiles from the deep orange solution were removed under reduced pressure, and the resultant solid was washed with diethyl ether. The crude product was recrystallized from DMA by layering with diethyl ether. Deep yellow-orange microcrystals were isolated after filtration, washed with diethyl ether, and dried in vacuo to give the titled salt in 66% yield (0.16 g).

With 4-Methylmorpholine-*N*-oxide (mmNO): This reaction was done as described above with Me_3NO and the following quantities of reagents: H_6**1** (0.175 g, 0.395 mmol), KH (0.064 g, 1.6 mmol), $Fe(OAc)_2$ (0.069 g, 0.40 mmol), and mmNO (0.048 g, 0.41 mmol). After the addition of MNO, the reaction was stirred for 1 h. The recrystallized metal salt was isolated in 50% yield (0.117 g). GC analysis confirmed the production of *N*-methylmorpholine as the organic product in 70% yield.

With Pyridine-*N*-oxide (pyNO): This reaction followed the above procedure using H_6**1** (0.190 g, 0.428 mmol), KH (0.069 g, 1.7 mmol), $Fe(OAc)_2$ (0.075 g, 0.43 mmol), and pyNO (0.042 g, 0.44 mmol). After the addition of pyNO, the reaction was stirred for 2 h. The deep orange-yellow salt of K_2[$Fe^{III}H_3$**1**(O)] was isolated in 55% yield (0.14 g) after recrystallization. GC analysis was used to establish a 70% yield of pyridine.

Preparation of K_2[$Mn^{III}H_3$1(O)]. With Me_3NO: This salt was synthesized using H_6**1** (0.200 g, 0.451 mmol), KH (0.072 g, 1.8 mmol), $Mn(OAc)_2$ (0.078 g, 0.45 mmol), and Me_3NO (0.036 g, 0.48 mmol) following the procedure outlined for K_2[$Fe^{III}H_3$**1**(O)] with Me_3NO. The reaction was stirred for 6 h after the addition of the *N*-oxide. The recrystallized metal salt was isolated in 67% yield (0.18 g).

With mmNO: The above procedure was used with H_6**1** (0.200 g, 0.451 mmol), KH (0.072 g, 1.8 mmol), $Mn(OAc)_2$ (0.078 g, 0.45 mmol), and mmNO (0.060 g, 0.51 mmol), and the reaction was stirred for 15 h at room temperature. K_2[$Mn^{III}H_3$**1**(O)] was isolated after recrystallization in 70% yield (0.19 g).

Preparation of K[$Fe^{III}H_3$1(OH)]. With Me_3NO: H_6**1** (0.220 g, 0.500 mmol) was treated with solid KH (0.060 g, 1.5 mmol) in ~12 mL of DMA under an argon atmosphere. The mixture was stirred until hydrogen gas evolution ceased, followed by the addition of solid $Fe(OAc)_2$ (0.087 g, 0.50 mmol). KOAc was filtered off from the reaction mixture. To the resulting pale yellow filtrate, Me_3NO (0.042 g, 0.56 mmol) was added, and the reaction mixture was stirred for 1 h. The crude compound was isolated after solvent removal under reduced pressure followed by being washed with diethyl ether. This salt was recrystallized from MeCN after layering with diethyl ether. Fine dark red microcrystalline product was isolated after filtration, washed with diethyl ether, and finally dried under *vacuum* to give K[$Fe^{III}H_3$**1**(OH)] in 60% yield (0.17 g).

With mmNO: This reaction was done in a similar manner as utilized for the Me_3NO reactions, employing H_6**1** (0.200 g, 0.451 mmol), KH (0.054 g, 1.4 mmol), $Fe(OAc)_2$ (0.079 g, 0.45 mmol), and mmNO (0.055 g, 0.47 mmol). The reaction was stirred for 3 h at room temperature after the addition of Me_3NO. K[$Fe^{III}H_3$**1**(OH)] was isolated in 65% yield (0.16 g), and *N*-methylmorpholine was produced in 78% yield as determined by GC analysis on an aliquot of the reaction mixture. This sample was analyzed after passing through a short silica gel plug.

With pyNO. This reaction used PyNO as the oxidant with the following amounts of reagents: H_6**1** (0.200 g, 0.451 mmol), KH (0.054 g, 1.4 mmol), $Fe(OAc)_2$ (0.079 g, 0.45 mmol), and pyNO (0.045 g, 0.47 mmol). After being stirred for 3 h at room temperature and workup, the final salt was isolated in a 62% (0.15 g) recrystallized yield and pyridine in a 66% yield, as determined by GC.

Preparation of K[$Mn^{III}H_3$1(OH)]. With Me_3NO: Following the method used for K[$Fe^{III}H_3$**1**(OH)] with *N*-oxides, K[$Mn^{III}H_3$**1**(OH)] was prepared starting with H_6**1** (0.175 g, 0.395 mmol), KH (0.048 g, 1.2 mmol), $Mn(OAc)_2$ (0.068 g, 0.40 mmol), and Me_3NO (0.030 g, 0.40 mmol). After the addition of Me_3NO, the reaction was stirred for 6 h at room temperature. The salt was isolated in 65% recrystallized yield (0.14 g).

With mmNO: Following the same procedure as above and using H_6**1** (0.175 g, 0.40 mmol), KH (0.048 g, 1.184 mmol), $Mn(OAc)_2$ (0.068 g, 0.40 mmol), and mmNO (0.050 g, 0.43 mmol), the reaction was stirred for 15 h at room temperature. K[$Mn^{III}H_3$**1**(OH)] was obtained in 58% yield (0.13 g).

Syntheses with Hydroxylamines. K_2[$Fe^{III}H_3$1(O)]: The reaction used H_6**1** (0.200 g, 0.451 mmol), KH (0.072 g, 1.8 mmol), $Fe(OAc)_2$ (0.079 g, 0.45 mmol), and *N*,*N*-diethylhydroxylamine (DEHA) (0.041 g, 0.46 mmol) and was stirred for 2 h at room temperature after the addition of the DEHA. Workup and recrystallization of the salt following the previously described procedure yielded 0.13 g (48% yield) of product.

K[$Fe^{III}H_3$1(OH)]: This reaction was performed in the same way as above with the following changes: H_6**1** (0.150 g, 0.338 mmol), KH (0.041 g, 1.0 mmol), $Fe(OAc)_2$ (0.059 g, 0.34 mmol), and DEHA (0.030 g, 0.34 mmol) were used, and the reaction was stirred for 3 h after addition of DEHA. Recrystallized salt was isolated in 48% yield (0.090 g).

Syntheses with Sulfoxides. Preparation of K_2[$Fe^{III}H_3$1(O)]. With DMSO: The reaction was done following the procedure outlined for the *N*-oxide reactions using H_6**1** (0.200 g, 0.451 mmol), KH (0.072 g, 1.8 mmol), $Fe(OAc)_2$ (0.079 g, 0.45 mmol), and DMSO (0.705 g, 9.02 mmol). The reaction was stirred for 3 h at room temperature. The crude salt was recrystallized from DMA after layering with diethyl ether to afford K_2[$Fe^{III}H_3$**1**(O)] in 60% yield (0.16 g).

With Diphenylsulfoxide (DPSO): This synthesis used the above procedure with H_6**1** (0.200 g, 0.451 mmol), KH (0.072 g, 1.8 mmol), $Fe(OAc)_2$ (0.079 g, 0.45 mmol), and DPSO (0.548 g, 2.71 mmol). The reaction was stirred for 15 h at room temperature. K_2[$Fe^{III}H_3$**1**(O)] was isolated in 64% (0.17 g) recrystallized yield. Diphenylsulfide as the organic product was confirmed by GC analysis in 65% yield.

Preparation of K[$Fe^{III}H_3$1**(OH)]. With DMSO:** This reaction was done using a similar procedure as described above for the generation of the Fe^{III}−O complexes with the following modifications: H_6**1** (0.200 g, 0.451 mmol), KH (0.054 g, 1.4 mmol), $Fe(OAc)_2$ (0.079 g, 0.45 mmol), and DMSO (0.705 g, 9.02 mmol). The reaction was stirred for 3 h at room temperature. Recrystallized salt was isolated in 64% (0.16 g) yield.

With DPSO: This reaction was done as above with H_6**1** (0.200 g, 0.451 mmol), KH (0.054 g, 1.4 mmol), $Fe(OAc)_2$ (0.079 g, 0.45 mmol), and DPSO (0.548 g, 2.71 mmol). The reaction was stirred for 15 h at room temperature. K[$Fe^{III}H_3$**1**(OH)] was isolated in 52% (0.13 g) recrystallized yield. Diphenylsulfide as the organic product was confirmed by GC analysis in 70% yield.

Physical Methods. Electronic spectra were recorded with a Cary 50 spectrophotometer. FTIR spectra were collected on a Mattson Genesis series FTIR instrument and are reported in wavenumbers. Room-temperature magnetic susceptibility measurements of solid samples were obtained using a MSB-1 magnetic susceptibility balance (Johnson Matthey). Diamagnetic corrections were taken from those reported by O'Connor.[28] Perpendicular-mode X-band EPR spectra were collected using a Bruker EMX spectrometer equipped with an ER041XG microwave bridge. Spectra for all EPR active samples were collected using the following spectrometer settings: attenuation = 25 dB, microwave power = 0.638 mW, frequency = 9.48 GHz, sweep width = 5000 G, modulation amplitude = 10.02 G, gain = 8.93×10^{-3}, conversion time = 81.920 ms, time constant = 327.68 ms, and resolution = 1024 points. A quartz liquid nitrogen finger-dewar (Wilmad Glass) was used to record spectra at 77 K. Parallel-mode X-band EPR spectra were recorded on a Bruker ESP300 spectrometer equipped with an Oxford ESR910 cryostat and a bimodal cavity (Bruker ER4116DM). Mössbauer spectra were obtained on a constant acceleration instrument and isomeric shifts are reported relative to an iron metal standard. GC analysis was done on a Hewlett-Packard 6890 Series gas chromatograph equipped with a HP 7683 Series injector. A calibration plot was established for the quantitative determination of organic products.

Density Functional Theory Calculations. Density functional theory (DFT) calculations for the H-bond cavities in [$Fe^{III}H_3$**1**(O)]$^{2-}$ and [$Mn^{III}H_3$**1**(O)]$^{2-}$ were carried out on model complexes that replaced the ureido *tert*-butyl groups with methyl groups. Using the structural coordinates obtained from X-ray diffraction studies, the geometries of the H-bond cavities, the M−O units, and the trigonal coordination planes (i.e., the ones containing the deprotonated α-nitrogen atoms) for each complex were optimized, while the ethylene groups and the amine nitrogen of the [H_3**1**]$^{3-}$ ligand were held fixed.[29] These constrained optimizations used the B3LYP functionals and the 6-31+G-(d,f) basis set.[30,31] All calculations were carried out using the Q-Chem 2.0 program.[32] To explore the energy of the complexes for different proton positions, constrained optimizations were also completed in which the oxo-proton distance was constrained. This allowed for the relative energies of the -oxo and -hydroxo forms of the complex to be estimated. We have found that the energy differences between different complex conformations obtained with these two functionals are within ∼1−2 kcal/mol.

The electronic structure and bonding in [$Fe^{III}H_3$**1**(O)]$^{2-}$ and [$Mn^{III}H_3$**1**(O)]$^{2-}$ were examined via quantum chemically generated orbital density plots and natural bond order (NBO)[33] population analysis. This was accomplished at the B3LYP/6-31G(d,f)[30] level using the Gaussian 98 suite of programs.[34] Spin state purity was ensured by constraining orbitals to a restricted open-shell form, and Boys localization[35] was performed to facilitate the interpretation of orbital density plots. Orbitals of interest were selected by choosing those valence eigenvectors with a Mulliken density on the metal atom that was at least 0.20 electrons (i.e., those for whom the sum of squares of metal basis function coefficients was at least 0.10).

Crystallography. General Methods. All crystals were attached to a glass fiber under nitrogen and mounted on a Siemens SMART system for data collection at 173(2) K. The data collection was carried out using Mo Kα radiation (graphite monochromator). The collection technique used for these samples is generally known as a hemisphere collection. The structures were solved by direct methods.[36] Several full-matrix least squares/difference Fourier cycles were performed, which located all non-hydrogen atoms. All non-hydrogen atoms were refined with anisotropic displacement parameters. Hydrogen atoms were placed in ideal positions and refined as riding atoms with relative isotropic displacement parameters. The methyl groups of the DMA solvates were converted to riding atoms prior to the final refinement. The urea NH protons were placed as ideal riding atoms. See Table 1 for additional crystal and refinement information.

Structure Solution and Refinements. K_2[$Fe^{III}H_3$1(O)]·4DMA and K_2[$Mn^{III}H_3$1(O)]·4DMA. For K_2[$Fe^{III}H_3$**1**(O)]·4DMA, the space group $P2_1/n$ was determined on the basis of systematic absences and intensity statistics. The unit cell was found to be primitive monoclinic, with *a* and *c* axes nearly the same length. This unit cell could be transformed to a *C*-centered orthorhombic cell with twice the volume, but this appeared to be coincidental. R_{int} for the corrected monoclinic cell was 0.054 while the *C*-centered orthorhombic cell was 0.167. These results suggested that pseudromerohedral twinning was present. The extent of this twinning was 11% by the 9 (row) [0 0 1/ 0−1 0/ 1 0 0] twin law. In this case, it appeared that reflections were not split appreciably. There were two independent molecules in the asymmetric unit denoted by "a" and "b". Anion b had one urea arm that was disordered, which was refined in a 0.48:0.52 ratio occupancy. FLAT and SAME restraints were applied along with appropriated displacement restraints. Each complex interacted with one potassium ion, while two potassium cations were bonded to two DMA solvates each and urea oxygens. This network formed pleated sheets, which reinforced the proposed pseudromerohedral twinning. Four other DMA molecules were coordinated to the two potassium cations. Two additional DMA solvates were present in the asymmetric unit. A pair of DMA molecules was disordered positionally over two sites. FLAT and SAME restraints were applied along with the appropriate displacement restraints. All atoms were refined with anisotropic displacements, and 924 restraints were used in total. The solution and refinement were analogous for K_2[$Mn^{III}H_3$**1**(O)]·

(28) O'Connor, C. J. *Prog. Inorg. Chem.* **1982**, *29*, 203−283.
(29) The geometric model used for these calculations was obtained from X-ray diffraction studies, where the broken symmetry was observed because of crystal packing interactions.
(30) (a) Ditchfield, R.; Hehre, W. J.; Pople, J. A. *J. Chem. Phys.* **1971**, *54*, 724−728. (b) Hehre, W. J.; Ditchfield, R.; Pople, J. A. *J. Chem. Phys.* **1972**, *56*, 2257−2261. (c) Francl, M. M.; Pietro, W. J.; Hehre, W. J.; Binkley, J. S.; Gordon, M. S.; DeFrees, D. J.; Pople, J. A. *J. Chem. Phys.* **1982**, *77*, 3654−3665.
(31) Diffuse functions are not used for the metal atoms.
(32) Kong, J.; White, C. A.; Krylov, A. I.; Sherrill, C. D.; Adamson, R. D.; Furlani, T. R.; Lee, M. S.; Lee, A. M.; Gwaltney, S. R.; Adams, T. R.; Ochsenfeld, C.; Gilbert, A. T. B.; Dedziora, G. S.; Rassolov, V. A.; Maurice, D. R.; Nair, N.; Shao, Y.; Besley, N. A.; Maslen, P. E.; Domboski, J. P.; Daschel, H.; Zhang, W.; Korambath, P. P.; Baker, J.; Byrd, E. F. C.; Van Voorhis, T.; Oumi, M.; Hirata, S.; Hsu, C.-P.; Ishikawa, N.; Florian, J.; Warshel A.; Johnson, B. G.; Gill, P. M. W.; Head-Gordon, M.; Pople, J. A. *J. Comput. Chem.* **2000**, *21*, 1532−1548.
(33) Reed, A. E.; Curtiss, L. A.; Weinhold, F. *Chem. Rev.* **1988**, *88*, 899−926 and references therein.
(34) Frisch, M. J.; Trucks, G. W.; Schlegel, H. B.; Scuseria, G. E.; Robb, M. A.; Cheeseman, J. R.; Zakrzewski, V. G.; Montgomery, J. A., Jr.; Stratmann, R. E.; Burant, J. C.; Dapprich, S.; Millam, J. M.; Daniels, A. D.; Kudin, K. N.; Strain, M. C.; Farkas, O.; Tomasi, J.; Barone, V.; Cossi, M.; Cammi, R.; Mennucci, B.; Pomelli, C.; Adamo, C.; Clifford, S.; Ochterski, J.; Petersson, G. A.; Ayala, P. Y.; Cui, Q.; Morokuma, K.; Malick, D. K.; Rabuck, A. D.; Raghavachari, K.; Foresman, J. B.; Cioslowski, J.; Ortiz, J. V.; Stefanov, B. B.; Liu, G.; Liashenko, A.; Piskorz, P.; Komaromi, I.; Gomperts, R.; Martin, R. L.; Fox, D. J.; Keith, T.; Al-Laham, M. A.; Peng, C. Y.; Nanayakkara, A.; Gonzalez, C.; Challacombe, M.; Gill, P. M. W.; Johnson, B. G.; Chen, W.; Wong, M. W.; Andres, J. L.; Head-Gordon, M.; Replogle, E. S.; Pople, J. A. *Gaussian 98*, revision x.x; Gaussian, Inc.: Pittsburgh, PA, 1998.
(35) Boys, S. F. *Rev. Mod. Phys.* **1960**, *32*, 296−299 and references therein.
(36) *SHELXLT-Plus*, version 6.1; Bruker Analytical X-ray Systems: Madison, WI.

Table 1. Crystallographic Data for $K_2[Fe^{III}H_3\mathbf{1}(O)]\cdot 4DMA$, $K_2[Mn^{III}H_3\mathbf{1}(O)]\cdot 4DMA$, $K[Fe^{III}H_3\mathbf{1}(OH)]\cdot 0.5CH_3CN$, and $K[Mn^{III}H_3\mathbf{1}(OH)]\cdot 0.5CH_3CN$

salt	$K_2[Fe^{III}H_3\mathbf{1}(O)]\cdot 4DMA$	$K_2[Mn^{III}H_3\mathbf{1}(O)]\cdot 4DMA$	$K[Fe^{III}H_3\mathbf{1}(OH)]\cdot 0.5CH_3CN$	$K[Mn^{III}H_3\mathbf{1}(OH)]\cdot 0.5CH_3CN$
molecular formula	$C_{37}H_{78}FeK_2N_{11}O_8$	$C_{37}H_{78}MnK_2N_{11}O_8$	$C_{22}H_{44.5}FeKN_{7.5}O_4$	$C_{22}H_{44.5}MnKN_{7.5}O_4$
fw	939.16	938.09	573.12	572.11
T (°C)	−100(2)	−100(2)	−100(2)	−100(2)
space group	$P2_1/n$	$P2_1/n$	$P\bar{1}$	$P\bar{1}$
a (Å)	30.586(2)	30.589(5)	10.7340(7)	10.715(2)
b (Å)	11.585(1)	11.6164(19)	18.3229(14)	18.284(3)
c (Å)	30.613(3)	30.605(5)	19.5249(13)	19.540(3)
α (deg)	90	90	74.261 92)	74.616(2)
β (deg)	107.954(2)	107.867(3)	89.088(1)	89.609(2)
γ (deg)	90	90	72.969(1)	73.021(2)
Z	8 ($Z' = 2$)	8 ($Z' = 2$)	4 ($Z' = 2$)	4 ($Z' = 2$)
V (Å^3)	10319(2)	10351(3)	3525.6(4)	3519.8(10)
δ_{calcd} (Mg/m^3)	1.209	1.204	1.080	1.080
R[a]	0.0724	0.0701	0.0436	0.0651
R_w[b]	0.1484	0.1629	0.1091	0.1433
GOF[c]	1.089	1.063	1.036	1.043

[a] $R = [\sum|\Delta F|/\sum|F_o|]$. [b] $R_w = [\sum\omega(\Delta F)^2/\sum\omega F_o^2]$. [c] Goodness of fit on F^2.

Scheme 1 [a]

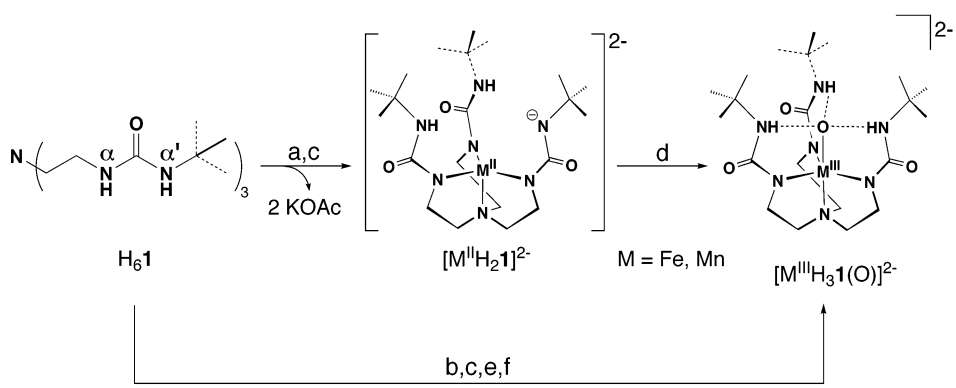

[a] Conditions: (a) 4 equiv KH, DMA, Ar, RT. (b) 5 equiv KH, DMA, Ar, RT. (c) $M(OAc)_2$, Ar, RT. (d) 0.5 equiv O_2, RT. (e) H_2O, RT. (f) $[Cp_2Fe]^+$ or I_2.

4DMF to yield a nearly identical unit cell and lattice structure. Pseudoromerohedral twinning was also observed in this structure, with the masses of the components being in a ratio of 0.64:0.36. One urea group was disordered (60:40 ratio) in anion B.

$K[Fe^{III}H_3\mathbf{1}(OH)]\cdot 0.5CH_3CN$ and $K[Mn^{III}H_3\mathbf{1}(OH)]\cdot 0.5CH_3CN$. These salts crystallized in the triclinic space group, $P\bar{1}$, with nearly identical unit cells. Both lattices had large channels that were parallel to the a axis that was filled with disordered solvent. PLATON/SQUEEZE[37] was used to evaluate the solvent channels and to correct the diffraction data for the effects of the diffuse scattering. For $K[Fe^{III}H_3\mathbf{1}(OH)]$, the solvent channel volume was 22% of the total volume (781 of 3520 Å^3), while in $K[Mn^{III}H_3\mathbf{1}(OH)]$ it was 23% (803 of 3526 Å^3).

Results and Discussion

Preparation of Complexes from Dioxygen. The synthesis of the $[M^{III}H_3\mathbf{1}(O)]^{2-}$ (M^{III} = Fe and Mn) from dioxygen is outlined in Scheme 1. A dimethylacetamide (DMA) solution of $H_6\mathbf{1}$ was treated with 4 equiv of KH under an Ar atmosphere. After H_2 evolution ceased, $M(OAc)_2$ was added as a solid in one portion, which resulted in the precipitation of 2 equiv of KOAc. The addition of half an equivalent of O_2 at room temperature produced an immediate color change of the reaction mixture to dark orange ($[Fe^{III}H_3\mathbf{1}(O)]^{2-}$) or deep brown ($[Mn^{III}H_3\mathbf{1}(O)]^{2-}$). Note that the presence of acetate ion does not appear to affect the oxidation of the M^{II} complex, and removal of the KOAc prior to oxidation does not affect the formation of the M^{III}−oxo complexes. The dipotassium salts of $[Fe^{III}H_3\mathbf{1}(O)]^{2-}$ and $[Mn^{III}H_3\mathbf{1}(O)]^{2-}$ are isolated in ca. 70% yield after recrystallization from DMA/diethyl ether. The preparations of these complexes are water sensitive, producing significant amounts of corresponding $[M^{III}H_3\mathbf{1}(OH)]^-$ complexes when wet reagents are employed. The $[M^{III}H_3\mathbf{1}(O)]^{2-}$ complexes are stable for weeks in the solid state when stored in a dry, anaerobic environment.

Scheme 2 illustrates the preparations of the $[M^{III}H_3\mathbf{1}(OH)]^-$ complexes from O_2, which afforded $[Fe^{III}H_3\mathbf{1}(OH)]^-$ and $[Mn^{III}H_3\mathbf{1}(OH)]^-$ in 60 and 52% yields after recrystallization. The synthetic procedures for the M^{III}−oxo and M^{III}−hydroxo are similar, with the major difference being the amount of base added to $H_6\mathbf{1}$. The synthesis of the M^{III}−hydroxo complexes utilizes 3 equiv of base, the amount necessary to deprotonate the αNH groups to form $[H_3\mathbf{1}]^{3-}$. Binding of metal ions to $[H_3\mathbf{1}]^{3-}$ produces complexes with three potential H-bond donors from the α′NH groups within the cavity (Scheme 2). The formation of the M^{III}−oxo complexes required an additional equivalent of base, which we propose serves to deprotonate one urea α′NH group to form $[H_2\mathbf{1}]^{4-}$. This produces complexes ($[M^{II}H_2\mathbf{1}]^{2-}$), whose cavities have two H-bond donors and one basic α′N$^-$ site (Scheme 1).

Support for this proposal comes from EPR measurements on solutions of $[Fe^{II}H_2\mathbf{1}]^{2-}$ and $[Fe^{II}H_3\mathbf{1}]^-$, which indicate that different amounts of added base produce distinct Fe^{II} precursors. Low-temperature (4 K) EPR spectra of $[Fe^{II}H_2\mathbf{1}]^{2-}$ and $[Fe^{II}H_3\mathbf{1}]^-$

(37) Spek, A. *Acta Crystallogr.* **1990**, *A46*, C-34.

Scheme 2 [a]

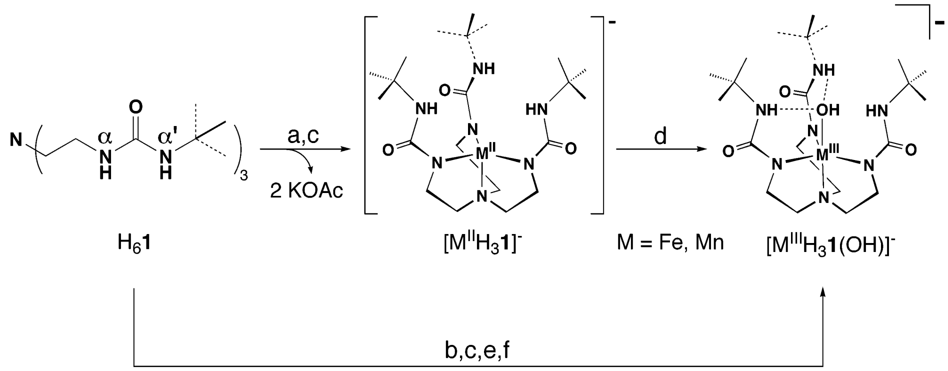

[a] Conditions: (a) 3 equiv KH, DMA, Ar, RT. (b) 4 equiv KH, DMA, Ar, RT. (c) $M(OAc)_2$, Ar, RT. (d) 0.5 equiv O_2, RT. (e) 1 equiv H_2O, RT. (f) [O].

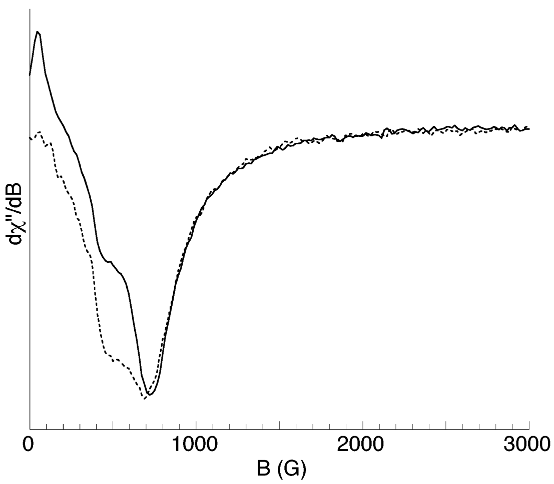

Figure 1. Parallel-mode X-band EPR spectra for $[Fe^{II}H_3\mathbf{1}]^-$ (−−−) and $[Fe^{II}H_2\mathbf{1}]^{2-}$ (- - -) recorded at 4 K.

in DMA for microwave fields polarized parallel to the static field are shown in Figure 1. $[Fe^{II}H_3\mathbf{1}]^-$ displays a signal at $g = 9$, while $[Fe^{II}H_2\mathbf{1}]^{2-}$ has a peak at a g-value of 9.6. The spectral intensities in Figure 1 have been arbitrarily adjusted to show the signal shift between the two complexes; however, for equal sample concentrations, the signal from $[Fe^{II}H_2\mathbf{1}]^{2-}$ is 3-fold more intense. The position and line shape of the signals are indicative of a high-spin Fe(II) state ($S = 2$), and variable temperature measurements indicate that the signals originate from the ground $m_s = \pm 2$ doublet, thus $D < 0$. The larger g-value and intensity for the spectrum of $[Fe^{II}H_2\mathbf{1}]^{2-}$ indicate an increase in the rhombic parameter E/D and, thus, lower symmetry around the iron center. This observation is consistent with the $[H_2\mathbf{1}]^{4-}$ ligand providing a more unsymmetrical environment around the iron center than $[H_3\mathbf{1}]^{3-}$. Low-temperature (4 K) Mössbauer spectra of $[Fe^{II}H_2\mathbf{1}]^{2-}$ and $[Fe^{II}H_3\mathbf{1}]^-$ in DMA in low magnetic field (45 mT) display only a single quadrupole doublet. Within the resolution of the doublets, both complexes display the same parameters: $\delta = 1.31$ mm/s, and $E_Q = 2.85$ mm/s. These parameters also are indicative of high-spin Fe(II) states for the complexes.

One possible function of the basic $\alpha'N^-$ site(s) is to scavenge protons produced during reaction. Consistent with this proposal is the preparation of the $M^{III}{-}O(H)$ complexes directly from water (Schemes 1 and 2).[19d,e] For the $M^{III}{-}O$ complexes, the reaction protocol involves treating $H_6\mathbf{1}$ with 5 equiv of base, $M^{II}(OAc)_2$, 1 equiv of water, and an oxidant such as I_2 or

Scheme 3 [a]

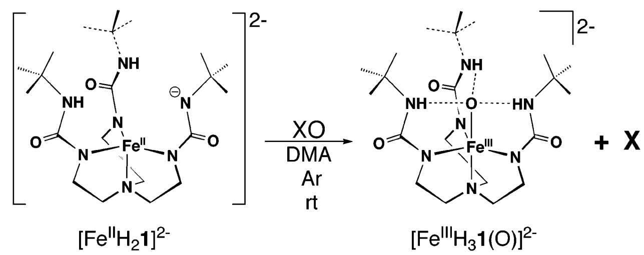

[a] XO = *N*-oxides, hydroxylamines, sulfoxides.

$[Cp_2Fe][BF_4]$. Recrystallized yields of ∼65% were obtained for $[M^{III}H_3\mathbf{1}(O)]^{2-}$, which are comparable to those obtained from dioxygen activation. A similar approach, but using 4 equiv of base, afforded $[M^{III}H_3\mathbf{1}(OH)]^-$ in satisfactory yields (Scheme 2).

Preparation of Complexes from Oxygen Atom Transfer Reagents. The $Fe^{III}{-}$oxo complexes can also be prepared in good yields from oxygen atom transfer agents (Scheme 3). For instance, treating $[Fe^{II}H_2\mathbf{1}]^{2-}$ with 1 equiv of Me_3NO produces $[Fe^{III}H_3\mathbf{1}(O)]^{2-}$ in 66% yield. Similarly, $[Fe^{III}H_3\mathbf{1}(O)]^{2-}$ was obtained in comparable yields with mmNO and pyNO, and GC analysis showed that 4-methyl-morpholine and pyridine were produced in 70% yields. Analogous results were obtained using Me_3NO and mmNO for the preparation of $[Mn^{III}H_3\mathbf{1}(O)]^{2-}$; however, the $Mn^{III}{-}O$ complexes were not formed when pyNO was the oxygen atom source. This lack of reactivity is explained by pyNO having a larger N−O bond dissociation energy than Me_3NO and mmNO.[1d] Finally, *N*,*N*-diethylhydroxylamine also produces the $[Fe^{III}H_3\mathbf{1}(O)]^{2-}$ in a yield of ∼50%.

A similar trend was observed in the formation of the $[M^{III}H_3\mathbf{1}(OH)]^-$ complexes. All the *N*-oxides discussed above can be used to prepare $[Fe^{III}H_3\mathbf{1}(OH)]^-$; however, only Me_3NO and mmNO produced $[Mn^{III}H_3\mathbf{1}(OH)]^-$. In addition, *N*,*N*-diethylhydroxylamine was used to produce the $[Fe^{III}H_3\mathbf{1}(OH)]^-$ in yields approaching 50%.

The $Fe^{III}{-}O(H)$ complexes were also prepared using sulfoxides. Treating $[Fe^{II}H_2\mathbf{1}]^{2-}$ and $[Fe^{II}H_3\mathbf{1}]^-$ with DMSO and DPSO affords $[Fe^{III}H_3\mathbf{1}(O)]^{2-}$ and $[Fe^{III}H_3\mathbf{1}(OH)]^-$ in isolated yields ranging from 52 to 64%. GC analysis of the reactions using DPSO showed that diphenylsulfide was also produced in a yield of greater than 60%. The use of sulfoxides as oxygen atom transfer reagents is well-known for second- and third-row transition-metal complexes.[1d] To our knowledge, this type of reactivity has not been reported for late 3d transition-metal complexes. These results underscore the strong affinity that these

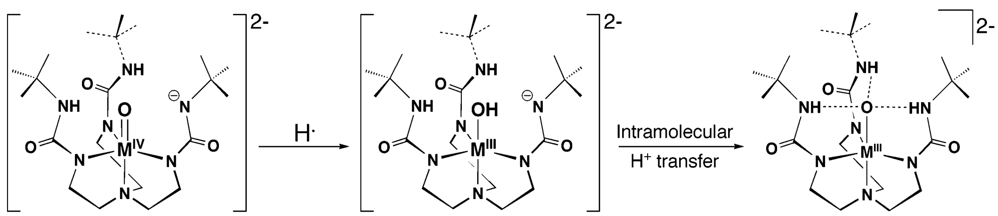

$[M^{IV}H_2\mathbf{1}(O)]^{2-}$ $[M^{III}H_2\mathbf{1}(OH)]^{2-}$ $[M^{III}H_3\mathbf{1}(O)]^{2-}$

Figure 2. Proposed intermediates in the formation of $[M^{III}H_3\mathbf{1}(O)]^{2-}$ (M^{III} = Fe and Mn).

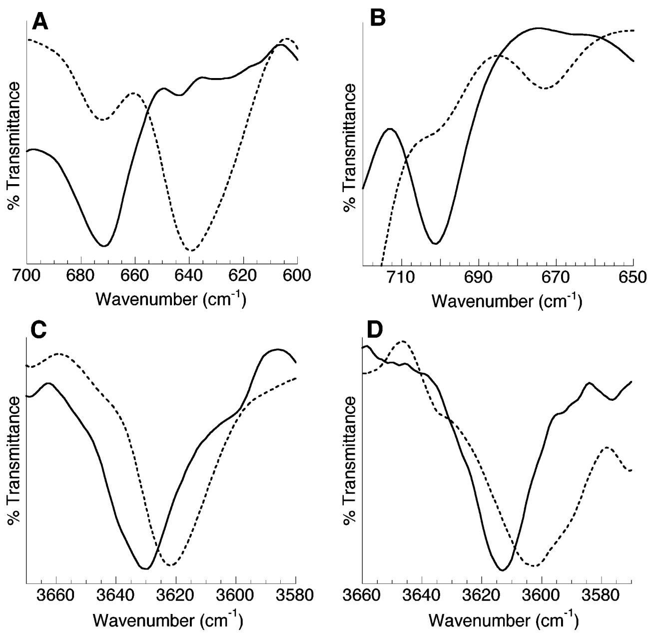

Figure 3. FTIR spectra of $[Fe^{III}H_3\mathbf{1}(O)]^{2-}$ (A), $[Mn^{III}H_3\mathbf{1}(O)]^{2-}$ (B), $[Fe^{III}H_3\mathbf{1}(OH)]^{-}$ (C), and $[Mn^{III}H_3\mathbf{1}(OH)]^{-}$ (D). Solid-line spectra are complexes derived from $^{16}O_2$, and dashed-lined spectra are those from $^{18}O_2$.

iron and manganese systems have for oxygen atoms, particular the Fe^{II} complexes.

Mechanistic Considerations. A partial mechanism in agreement with these results is proposed for the formation of the $M^{III}-O$ complexes (Figure 2). The oxygen atom transfer studies suggest the production of $M^{IV}-O$ intermediates, which we have shown are competent to abstract hydrogen atoms from external species, such as solvent.[38] The resultant species, $[M^{III}H_2\mathbf{1}(OH)]^{2-}$, contains a basic $\alpha'N^-$ within the cavity, positioned proximally to the coordinated hydroxo ligand. Intramolecular proton transfer between the endogenous basic site and the $M^{III}-OH$ unit yields the $M^{III}-O$ complexes.

Vibrational and Isotopic Labeling Studies. The $M^{III}-$oxo complexes have distinguishable vibrational features that have allowed us to determine that O_2 was the source of the terminal oxo ligands. For $[Fe^{III}H_3\mathbf{1}(O)]^{2-}$, Fourier transform infrared experiments revealed a peak at 671 cm^{-1}, which is assigned to the Fe$-$O vibration (Figure 3). This peak shifts to 645 cm^{-1} in the FTIR spectrum of $[Fe^{III}H_3\mathbf{1}(^{18}O)]^{2-}$. The observed difference of 26 cm^{-1} in Fe$-$O vibrations for the two Fe$-$O isotopomers is expected on the basis of a simple harmonic Fe$-$O oscillator model. Similar findings were observed for $[Mn^{III}H_3\mathbf{1}(O)]^{2-}$: a ν(Mn$-^{16}$O) of 700 cm^{-1} was found for $[Mn^{III}H_3\mathbf{1}(^{16}O)]^{2-}$, which shifts the expected amount to 672 cm^{-1} in $[Mn^{III}H_3\mathbf{1}(^{18}O)]^{2-}$. Both Fe and Mn$-^{18}$O isotopomers were prepared using the method shown in Scheme 1 and $^{18}O_2$.

The Fe$-$O vibration at 671 cm^{-1} for $[Fe^{III}H_3\mathbf{1}(^{16}O)]^{2-}$ occurs outside the range reported for heme and non-heme $Fe^{IV}-O$ systems; for instance, a ν(Fe$-$O) of 834 cm^{-1} was found for the monomeric $Fe^{IV}-O$ complex $[Fe^{IV}(tmc)(O)(CH_3CN)]^{2+}$.[10,39] Furthermore, monomeric Mn^{IV} and Mn^{V} complexes with terminal oxo ligands have stronger Mn$-$O vibrations than the 700 cm^{-1} feature found for $[Mn^{III}H_3\mathbf{1}(^{16}O)]^{2-}$. A ν(Mn$-^{16}$O) of 754 cm^{-1} was reported for $Mn^{IV}-O$ porphyrins,[40] and Collins et al. have shown that square pyramidal $Mn^{V}-O$ complexes have Mn$-$O vibrations at 979 cm^{-1}.[9b] The energies of Mn$-$O vibrations associated with these higher valent complexes have been attributed to multiple bonds between the manganese and oxo ions.

Isotopic labeling studies also confirmed that the oxygen atoms in the hydroxo ligands of $[Fe^{III}H_3\mathbf{1}(OH)]^{-}$ and $[Mn^{III}H_3\mathbf{1}(OH)]^{-}$ are derived directly from O_2. The FTIR spectrum of $[Fe^{III}H_3\mathbf{1}(^{16}OH)]^{-}$ reveals a ν(Fe^{16}O$-$H) at 3632 cm^{-1}, which shifts to 3621 cm^{-1} in $[Fe^{III}H_3\mathbf{1}(^{18}OH)]^{-}$ (FTIR: $\nu(^{16}OH)/\nu(^{18}OH) = 1.004$; calcd 1.003). For $[Mn^{III}H_3\mathbf{1}(OH)]^{-}$, the ν(Mn^{16}O$-$H) occurs at 3614 cm^{-1} and shifts the predicted amount to 3603 cm^{-1} in the ^{18}OH isotopomer. The vibrational properties in $[Mn^{III}H_3\mathbf{1}(OH)]^{-}$ resemble those found in $[Mn^{III}(tcca)(OH)]^{-}$,[39] another five-coordinate Mn^{III} complex with a terminal hydroxo ligand.[41] Note that as expected, the O$-$H vibrational features associated with the hydroxo ligands are absent in the FTIR spectra of the oxometal complexes, $[Fe^{III}H_3\mathbf{1}(O)]^{2-}$ and $[Mn^{III}H_3\mathbf{1}(O)]^{2-}$.

Structural Studies. Single-crystal X-ray diffraction methods were used to probe the solid-state molecular structures of the $M^{III}-O(H)$ complexes. Crystal, data collection, and refinement parameters are presented in Table 1. Single crystals of the complexes were grown as potassium salts and contained two crystallographically independent, yet virtually identical, anions in the asymmetric unit (denoted “A” and “B”). Metrical data for all the anions are found in Table 2; average metrical values will be used in the following descriptions of the structures.

All the complexes have trigonal bipyramidal coordination geometry as shown in Figure 4 for $[Fe^{III}H_3\mathbf{1}(O)]^{2-}$ and $[Fe^{III}H_3\mathbf{1}(OH)]^{-}$. The three deprotonated α-nitrogen atoms, N2, N4, and N6, of $[H_3\mathbf{1}]^{3-}$ define the trigonal plane with the apical amine nitrogen N1 and O1, the oxo or oxygen atom of the hydroxo ligand, occupying the axial positions. The remaining

(38) Gupta, R.; Borovik, A. S. *J. Am. Chem. Soc.* **2003**, *125*, 13234−13242.

(39) Abbreviations: tmc, 1,4,8,11-tetramethyl-1,4,8,11-tetraazacyclotetradecane; tcca, tris(cyclo-pentylcarbamoymethyl)aminato; tnpa, tris(6-neopentylamin-2-pyridylmethyl)amine; 5-NO_2-sal-*N*-mdpt, bis(2-hydroxy-5-nitrobenzylimi-nopropyl)methylamine.

(40) Czernuszewicz, R. S.; Su, Y. O.; Stern, M. K.; Macor, K. A.; Kim, D.; Groves, J. T.; Spiro, T. G. *J. Am. Chem. Soc.* **1988**, *110*, 4158−4165.

(41) Shirin, Z.; Young, V. G.; Borovik, A. S. *Chem. Commun.* **1997**, *4*, 1967−1968.

Table 2. Selected Bond Distances and Angles for $[Fe^{III}H_3\mathbf{1}(O)]^{2-}$, $[Mn^{III}H_3\mathbf{1}(O)]^{2-}$, $[Fe^{III}H_3\mathbf{1}((OH)]^{-}$, and $[Mn^{III}H_3\mathbf{1}((OH)]^{-}$ [a,b]

distance (Å) or angle (deg)	$[Fe^{III}H_3\mathbf{1}(O)]^{2-}$	$[Mn^{III}H_3\mathbf{1}(O)]^{2-}$	$[Fe^{III}H_3\mathbf{1}(OH)]^{-}$	$[Mn^{III}H_3\mathbf{1}(OH)]^{-}$
M1A−N1A	2.280(4)	2.141(5)	2.171(2)	2.023(3)
M1B−N1B	2.271(4)	2.147(5)	2.188(2)	2.042(3)
M1A−N2A	2.036(4)	2.047(5)	2.025(2)	2.036(3)
M1B−N2B	2.030(4)	2.056(5)	2.024(2)	2.026(3)
M1A−N4A	2.070(5)	2.102(5)	1.979(2)	2.073(3)
M1B−N4B	2.060(4)	2.107(4)	2.035(2)	2.079(3)
M1A−N6A	2.062(5)	2.062(5)	2.044(2)	2.013(3)
M1B−N6B	2.082(4)	2.135(4)	1.989(2)	2.016(3)
M1A−O1A	1.813(3)	1.780(5)	1.9315(17)	1.877(2)
M1B−O1B	1.813(3)	1.762(4)	1.9212(17)	1.868(2)
O1A···N3A	2.732(5)	2.733(8)	2.890(3)	2.783(4)
O1B···N3B	2.771(16)	2.776(9)	2.839(3)	2.831(4)
O1A···N5A	2.702(6)	2.722(7)	2.823(3)	2.876(4)
O1B···N5B	2.671(6)	2.693(6)	2.832(3)	2.871(4)
O1A···N7A	2.686(7)	2.732(7)	2.802(3)	2.893(4)
O1B···N7B	2.705(6)	2.729(6)	2.814(3)	2.840(4)
N1A−M1A−O1A	177.9(2)	178.1(2)	174.20(8)	176.41(11)
N1B−M1B−O1B	177.6(2)	177.4(2)	175.59(8)	177.84(10)
N2A−M1A−N4A	117.7(2)	120.1(2)	109.40(9)	113.45(11)
N2B−M1B−N4B	120.1(2)	123.01(18)	127.70(9)	109.86(11)
N2A−M1A−N6A	121.6(2)	124.7(2)	128.17(8)	134.84(11)
N2B−M1B−N6B	119.5(2)	121.44(18)	111.85(9)	134.68(11)
N4A−M1A−N6A	109.2(2)	108.2(2)	114.00(9)	106.13(11)
N4B−M1B−N6B	109.1(2)	108.11(18)	112.02(9)	110.18(11)
N1A−M1A−N2A	78.8(2)	81.62(19)	78.89(8)	82.73(11)
N1B−M1B−N2B	78.91(14)	81.21(18)	79.09(8)	83.01(11)
N1A−M1A−N4A	78.8(2)	81.34(18)	83.02(8)	83.47(11)
N1B−M1B−N4B	78.6(2)	80.62(17)	79.89(8)	82.88(10)
N1A−M1A−N6A	78.2(2)	80.51(19)	79.63(8)	80.97(11)
N1B−M1B−N6B	78.5(2)	80.86(17)	82.41(8)	81.73(11)

[a] There are two independent anions in the asymmetric unit for the complexes. Metrical parameters for both are reported. [b] The standard errors in the metrical parameters are slightly underestimated because of crystallographic twinning.

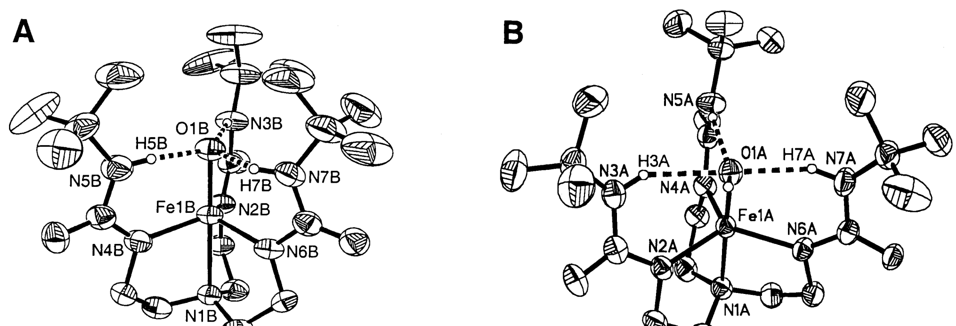

Figure 4. Thermal ellipsoid diagram of $[Fe^{III}H_3\mathbf{1}\text{-}\mathbf{b}(O)]^{2-}$ (A) and $[Fe^{III}H_3\mathbf{1}\text{-}\mathbf{a}(OH)]^{-}$ (B). The ellipsoids are drawn at the 50% probability level, and only the urea hydrogen atoms are shown. For $[Fe^{III}H_3\mathbf{1}\text{-}\mathbf{b}(O)]^{2-}$, only one of the disordered fragments for the arm containing N2b is shown.

components of the ureas are positioned nearly perpendicular to the trigonal plane, thus serving as scaffolding for a cavity surrounding the M−O(H) units. In each structure, the three α′NH groups are disposed within the cavity, toward the coordinated oxygen atom, with α′N···O1 distances of less than 2.9 Å (Table 2), which are indicative of intramolecular H-bonds. Solid-state FTIR experiments on crystalline samples corroborate the presence of H-bonds: the peaks for the N−H vibrations are broad and at lower energies (3250−3100 cm^{-1}) compared to systems not possessing H-bonds. The structure analyzed also shows that all the complexes are monomeric, a result of the H-bond cavity sufficiently confining the M−O(H) unit to prohibit intermolecular interactions with other metal complexes.

An Fe1−O bond length of 1.813(3) Å is observed in $[Fe^{III}H_3\mathbf{1}(O)]^{2-}$. This distance is comparable to those found for complexes with $Fe^{III}-O-Fe^{III}$ motifs.[12a] However, it is significantly longer than those reported for other systems with terminal Fe−O units. In $[Fe^{IV}(tmc)(O)(CH_3CN)]^{2+}$, the Fe−O distance is 1.646(3) Å,[10,39] while a 1.666(2) length is found in $[Fe^{VI}(O)_4]^{2-}$.[42] In addition, extended X-ray absorption fine structure (EXAFS)[43] and low-resolution X-ray diffraction studies on heme protein show that $Fe^{IV}-O$ distances are less than 1.7 Å.[15,44] The longer Fe1−O1 bond in $[Fe^{III}H_3\mathbf{1}(O)]^{2-}$ likely reflects the trivalent oxidation state of the iron center and the H-bond network that surrounds the oxo ligand.

In the analogous $Fe^{III}-OH$ complex, $[Fe^{III}H_3\mathbf{1}(OH)]^{-}$, the Fe1−O1 length is 1.9264(17) Å, an increase of 0.113 Å compared to that in $[Fe^{III}H_3\mathbf{1}(O)]^{2-}$. Moreover, the Fe1−N1 distance of 2.180(2) Å in $[Fe^{III}H_3\mathbf{1}(OH)]^{-}$ is nearly 0.1 Å shorter than the corresponding bond length in $[Fe^{III}H_3\mathbf{1}(O)]^{2-}$. This is in agreement with an oxo donor having a stronger trans influence than a hydroxo ligand. The Fe1−O1 length in $[Fe^{III}H_3\mathbf{1}(OH)]^{-}$

(42) Hopper, M. L.; Schlemper, E. O.; Murmann, R. K. *Acta Crystallogr.* **1982**, *B32*, 2237−2240.
(43) (a) Penner-Hahn, J. E.; Eble, K. S.; McMurry, T. J.; Renner, M.; Balch, A. L.; Groves, J. T.; Dawson, J. H.; Hodgson, K. O. *J. Am. Chem. Soc.* **1986**, *108*, 7819−7825. (b) Anderson, L. A.; Dawson, J. H. *Struct. Bonding* **1991**, *74*, 1−40.
(44) Edwards, S. L.; Xuong, N. H.; Hamlin, R. C.; Kraut, J. *Biochemistry* **1987**, *26*, 1503−1511.

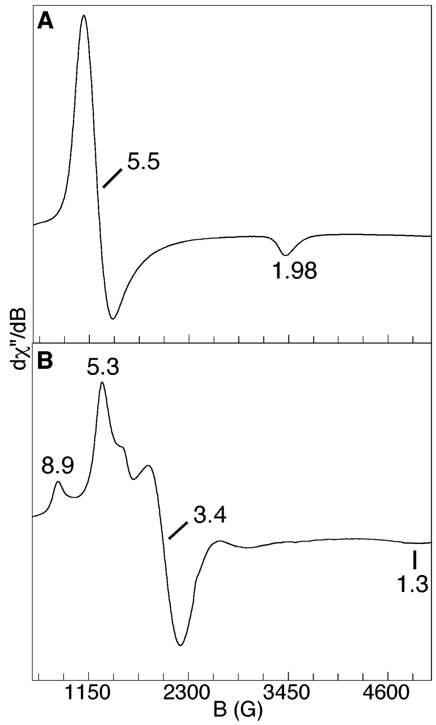

Figure 5. Perpendicular-mode X-band EPR spectra for $[Fe^{III}H_3\mathbf{1}(O)]^{2-}$ (A) and $[Fe^{III}H_3\mathbf{1}(OH)]^{-}$ (B) measured at 77 K. A small impurity giving rise to a signal at $g = 4.3$ is also observed.

is longer than the ∼1.88 Å distance found for the same bonds in ferric soybean lipoxygenase[45] and $[Fe(tnpa)(OH)(\eta^1\text{-}OAc)]^+$.[39,46] These latter systems have H-bond networks surrounding the Fe^{III}−OH units, but they differ from $[Fe^{III}H_3\mathbf{1}(OH)]^{-}$ by also having the hydroxo ligand H-bonded to a carboxyl group (i.e., OH···O═C). This additional H-bond interaction could lead to the shorter Fe−O(H) bond in the other complexes.

The presence of the hydroxo ligand in $[Fe^{III}H_3\mathbf{1}(OH)]^{-}$ causes greater distortions in the H-bond cavity and ligand geometry compared to $[Fe^{III}H_3\mathbf{1}(O)]^{2-}$. There is greater spread in the trigonal angles in $[Fe^{III}H_3\mathbf{1}(OH)]^{-}$ (Table 2), including a large N2−Fe1−N6 angle of 127.94(8)°. The lengthening of this angle results from the disposition of the O1−H1 bond between the two urea groups containing N2 and N6, indicating that a "stretching" of the cavity must occur to accommodate the nonspherical hydroxo ligand. EPR experiments provide further support for the differences in ligand geometry between $[Fe^{III}H_3\mathbf{1}(O)]^{2-}$ and $[Fe^{III}H_3\mathbf{1}(OH)]^{-}$. Frozen DMA solutions of $[Fe^{III}H_3\mathbf{1}(O)]^{2-}$ have an axial X-band EPR spectrum at 77 K with *g*-values of 5.5 and 1.98, producing a rhombic splitting parameter (E/D) of zero (Figure 5). In contrast, DMA solutions of $[Fe^{III}H_3\mathbf{1}(OH)]^{-}$ give a more complex X-band EPR spectrum with *g*-values of 8.9, 5.3, 3.4, and 1.3. These values yield an E/D of 0.17—a value consistent with $[Fe^{III}H_3\mathbf{1}(OH)]^{-}$ having a more distorted ligand field.

Similar structural trends are observed for Mn^{III}−O(H) complexes. $[Mn^{III}H_3\mathbf{1}(O)]^{2-}$ has an average Mn1−O1 length of 1.771(5) Å, which is significantly longer than the ∼1.60 Å distances reported for the monomeric Mn^{V}(oxo) tetraamidate complexes,[9a−b,11] but falls within the range found for Mn^{III}−O−Mn^{III} complexes.[12b] Consistent with FTIR measurements, the Mn1−O1 distance is shorter, by 0.042 Å, than the analogous Fe1−O1 length in $[Fe^{III}H_3\mathbf{1}(O)]^{2-}$. In $[Mn^{III}H_3\mathbf{1}(OH)]^{-}$, the Mn1−O1 distance lengthens to 1.873(2) Å and has a shorter Mn−N1 distance of 2.033(3) Å compared to that in $[Mn^{III}H_3\mathbf{1}(O)]^{2-}$ (2.144 (5) Å). The Mn1−O1 distance in $[Mn^{III}H_3\mathbf{1}(OH)]^{-}$ is also greater than those found in the other monomeric Mn^{III}−OH complexes, $[Mn^{III}(tcca)(OH)]^{-}$ (1.816(4) Å)[39,41] and Mn(5-NO_2-sal-*N*-mdpt)(OH) (1.827(3) Å),[39,47] both of which lack intramolecular H-bonds. The longer bond length in $[Mn^{III}H_3\mathbf{1}(OH)]^{-}$ is ascribed to its H-bond network around the MnOH unit, which should lead to an increase in the M−O(H) distance. A similar trend in M−O(H) bond lengths has been observed for related $[M^{II}H_3\mathbf{1}(OH)]^{2-}$ complexes (M^{II} = Mn, Fe, Co, and Zn).[19d]

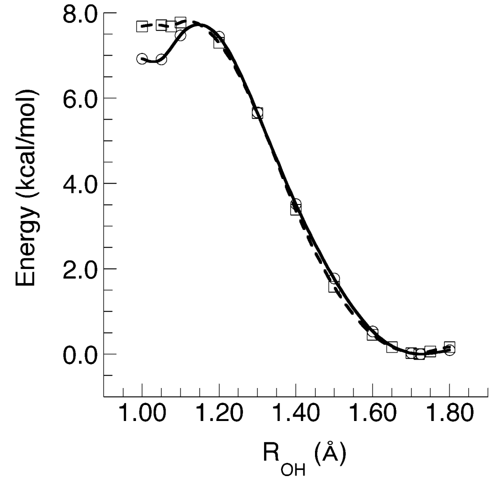

Figure 6. The energies of $[Fe^{III}H_3\mathbf{1}(O)]^{2-}$ (○, solid line) and $[Mn^{III}H_3\mathbf{1}(O)]^{2-}$ (□, dashed line) obtained from B3LYP/6-31+G* constrained optimization plotted versus MO···H (R_{OH}) distance. The lines are the best fit through the calculated points.

DFT Calculation: Cavity Studies. DFT calculations have been used to further probe the position of the ureido protons within the H-bond cavity in $[Fe^{III}H_3\mathbf{1}(O)]^{2-}$ and $[Mn^{III}H_3\mathbf{1}(O)]^{2-}$. The tautomers in eq 1 represent two limiting forms, α′NH···O−M^{III} (**A**) and α′N···HO−M^{III} (**B**), for placement of a proton between the oxo ligand and one of the α′NH groups. Our computational studies examined the energy difference between **A** and **B**. To further evaluate these theoretical results, the coordination geometries obtained from the DFT calculations were compared to those determined from X-ray diffraction data.

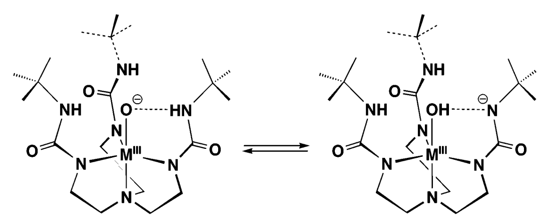

A **B** (1)

The constrained optimization on modified structures (see Experimental Section) of $[Fe^{III}H_3\mathbf{1}(O)]^{2-}$ and $[Mn^{III}H_3\mathbf{1}(O)]^{2-}$

(45) (a) Scarrow, R. C.; Trimitsis, M. G.; Buck, C. P.; Grove, G. N.; Cowling, R. A.; Nelson, M. J. *Biochemistry* **1994**, *33*, 15023−15035. (b) Tomchick, D. R.; Phan, P.; Cymborowski, M.; Minor, W.; Holman, T. R. *Biochemistry* **2001**, *40*, 7509−7517.
(46) Ogo, S.; Wada, S.; Watanabe, Y.; Iwase, M.; Wada, A.; Harata, M.; Jitsukawa, K.; Masuda, H.; Einage, H. *Angew. Chem., Int. Ed.* **1998**, *37*, 2102−2104.
(47) Eichhorn, D. M.; Armstrong, W. H. *J. Chem. Soc., Chem. Commun.* **1992**, 85−87.

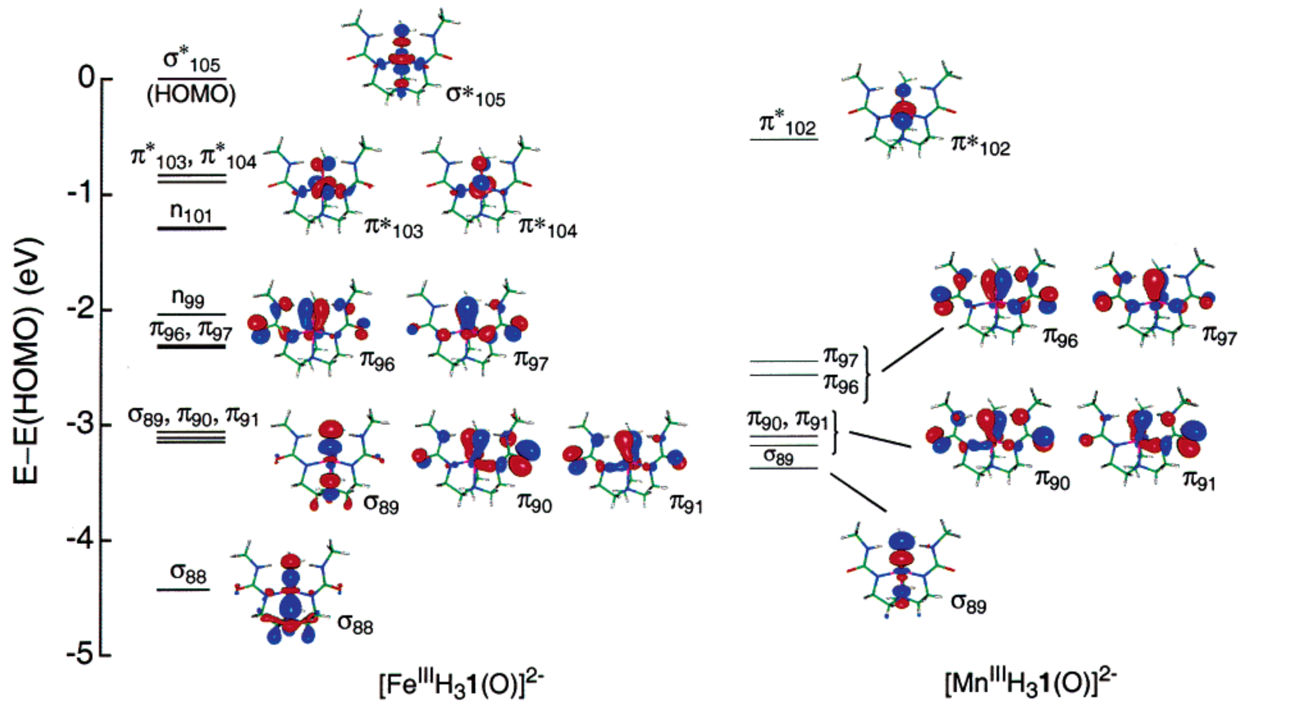

Figure 7. Theoretically derived molecular orbital energy level diagrams and corresponding plot for orbitals pertaining to the $M^{III}-O$ bonds in $[Fe^{III}H_3\mathbf{1}(O)]^{2-}$ and $[Mn^{III}H_3\mathbf{1}(O)]^{2}$. Orbitals listed include the lowest unoccupied MO plus all valence MOs with a Mulliken population of at least 0.10 arising from metal basis functions. The isosurfaces of the MOs correspond to wave function values of 0.05, with blue lobes indicating regions of positive parity and red lobes indicating regions of negative parity. The molecular structure is also depicted in stick form, with the Fe atom colored magenta and all other atoms rendered according to the usual CPK color scheme.

found that tautomer **A** has the lowest energy (Figure 6). For the iron system, the energy of **A** is 6.9 kcal/mol lower in energy than **B** (R_{OH} = 1.05 Å) at the B3LYP/6-31+G* level. At the same level of theory, the manganese system gives **A** 7.7 kcal/mol lower in energy. The optimized geometry of **A** gives an $Fe^{III}-O$ length of 1.792 Å, in excellent agreement with the distance of 1.813 Å obtained by X-ray diffraction (vide supra). A significantly longer distance of 1.875 Å is found for tautomer **B** of the iron system. For the manganese complexes, the experimentally determined $Mn^{III}-O$ distance is also closer to the bond length found for tautomer **A** (1.746 Å) than for **B** (1.812 Å).

The calculations also revealed that **A** and **B** have distinct differences in the separations between the oxo (or hydroxo oxygen atom) and the α′N atoms. The FeO···N distances in **A** are within 0.043 Å, at 2.750, 2.761, and 2.776 Å. The same span in distances was experimentally found for $[Fe^{III}H_3\mathbf{1}(O)]^{2-}$ (Table 2). In contrast, calculations on **B** yielded a range of 0.217 Å with FeO···N values of 2.635, 2.844, and 2.852 Å. A similar trend was found for the N–C–N–C dihedral angles of the urea groups.[48] Taken together, tautomer **B** clearly exhibits a more unsymmetrical H-bond cavity, which results from differences between the protonated and deprotonated urea groups. This large distortion was not observed in the molecular structure of $[Fe^{III}H_3\mathbf{1}(O)]^{2-}$ determined by X-ray diffraction and was not present in the calculated structure of tautomer **A**. Note that analogous findings were obtained for $[Mn^{III}H_3\mathbf{1}(O)]^{2-}$.

Bonding in $[M^{III}H_3\mathbf{1}(O)]^{2-}$. We have also used DFT to investigate the electronic structure in the $M^{III}-O$ complexes. Figure 7 contains the computationally derived molecular orbital energy level diagrams for orbitals with significant electron densities on the metal atom in $[Fe^{III}H_3\mathbf{1}(O)]^{2-}$ and $[Mn^{III}H_3\mathbf{1}(O)]^{2-}$.[49] There are a number of different molecular orbitals that appear to contribute to metal–oxo bond bonding: for $[Mn^{III}H_3\mathbf{1}(O)]^{2-}$ there are five bonding molecular orbitals plus one half-occupied antibonding orbital, while $[Fe^{III}H_3\mathbf{1}(O)]^{2-}$ has six molecular orbitals of bonding character and three half-occupied antibonding orbitals. However, this should not be construed to imply the presence of metal–oxo multiple bonds. As illustrated in Figure 7, and despite our use of the Boys localization scheme, none of these molecular orbitals have pure metal–oxo character; all the molecular orbitals have appreciable electron density elsewhere throughout the complex. Thus, the relative complexity of these molecular orbitals makes it difficult to approximate the net bond order of the metal–oxo bond solely from Figure 7.

Natural bond order (NBO) analyses were used to further investigate the bonding in $[Fe^{III}H_3\mathbf{1}(O)]^{2-}$ and $[Mn^{III}H_3\mathbf{1}(O)]^{2-}$; this method proved effective for deconvoluting the metal–oxo electron density and bonding properties. An NBO analysis of $[Fe^{III}H_3\mathbf{1}(O)]^{2-}$ gives an Fe–O σ-bond composed of 22.3% dz^2(Fe) + 77.7% pz(O) containing 1.939 electrons, while for $[Mn^{III}H_3\mathbf{1}(O)]^{2-}$, the Mn–O σ-bond is 2.9% s(Mn) + 20.0% dz^2(Mn) + 17.5% s(O) + 59.1% pz(O) with 1.987 electrons. These σ-bonds are partially offset in each complex by a small contribution from metal–oxo σ-antibonding molecular orbitals, amounting to 0.084 in $[Fe^{III}H_3\mathbf{1}(O)]^{2-}$ and 0.262 in $[Mn^{III}H_3\mathbf{1}(O)]^{2-}$.[50] The difference of bonding and antibonding molecular orbitals gives a M–O bond order of approximately

(48) N–C–N–C dihedral angles of 170.7°, 166.7°, and 165.5° were found for the urea arms by X-ray diffraction on $[Fe^{III}H_3\mathbf{1}(O)]^{2-}$; 162.4°, 162.4°, and 159.0° were calculated for tautomer **A**, and 179.9°, 163.0°, and 160.1° were calculated for tautomer **B**.

(49) Figure 7 contains MO plots for most of the orbitals used to construct the energy level diagrams.

0.92 in $[Fe^{III}H_3\mathbf{1}(O)]^{2-}$ and 0.86 in $[Mn^{III}H_3\mathbf{1}(O)]^{2-}$. The net contribution to the M−O bond is dominated by electrons associated with the oxo ligand, amounting to 87.3% in $[Fe^{III}H_3\mathbf{1}(O)]^{2-}$ and 77.1% for $[Mn^{III}H_3\mathbf{1}(O)]^{2-}$. The relative charges on the metal ions and their corresponding oxo oxygens are consistent with this finding.[51]

Summary and Conclusions

We have prepared and characterized a new series of mononuclear Fe^{III} and Mn^{III} complexes with terminal oxo and hydroxo ligands that are derived directly from dioxygen. The Fe^{III}−O(H) complexes, $[Fe^{III}H_3\mathbf{1}(O)]^{2-}$ and $[Fe^{III}H_3\mathbf{1}(OH)]^{-}$, were also synthesized using a variety of oxygen atom transfer agents, such as amine *N*-oxides and hydroxylamines; similar findings were observed for the related Mn^{III}−oxo complex, $[Mn^{III}H_3\mathbf{1}(O)]^{2-}$. The oxophilic character of these systems was further illustrated in the production of the Fe^{III}−O(H) complexes via oxygen atom transfer from sulfoxides, a reaction not observed previously in iron chemistry. Furthermore, the formation of the oxo and hydroxo complexes was dependent on the number of $\alpha'N^{-}$ groups generated within the cavity; these groups serve as endogenous bases for intramolecular proton transfer.

From these observations, a mechanism for the formation of the $[M^{III}H_3\mathbf{1}(O)]^{2-}$ complexes was proposed (Figure 2) and includes M^{IV}=O intermediates. Our previous studies on M^{III}O−H bond dissociation energies (BDE) suggest that the related $[Fe^{IV}H_3\mathbf{1}(O)]^{-}$ and $[Mn^{IV}H_3\mathbf{1}(O)]^{-}$ complexes have a large thermodynamic driving force for abstraction of a hydrogen atom, a requirement in our mechanism for the production of the M^{III}−O complexes.[38] In contrast, recent accounts show that Fe^{IV}=O complexes are somewhat stable,[10] even in the presence of solvents with relatively weak C−H bonds (e.g., CH_3CN: BDE_{CH} = 93 kcal/mol in DMSO).[52] Taken together, these findings indicate that the Fe^{IV}=O unit can have a variety of chemical reactivities.

The isolation of $[M^{III}H_3\mathbf{1}(O)]^{2-}$ and $[M^{III}H_3\mathbf{1}(OH)]^{-}$ was achieved using $[H_3\mathbf{1}]^{3-}$, a polydentate ligand designed to have a rigid organic cavity containing H-bond donors. Our studies confirmed the presence of intramolecular H-bonds, which are formed between the oxo or hydroxo ligands and the α'NH groups of $[H_3\mathbf{1}]^{3-}$. Moreover, spectroscopic, structural, and theoretical findings for $[Fe^{III}H_3\mathbf{1}(O)]^{2-}$ and $[Mn^{III}H_3\mathbf{1}(O)]^{2-}$ show that only a single σ-bond exists between the M^{III} centers and the oxo ligands;[53] the remaining interactions with the oxo ligands are provided by intramolecular H-bonds. This unusual arrangement of bonds provides compelling evidence that under certain circumstances H-bonds may replace π-bonds in stabilizing oxometal complexes.

These results reinforce the idea that reactivity of metal complexes may be regulated by H-bonds, a suggestion invoked for the activity of metalloproteins.[15,16,45b,54,55] The $[Fe^{III}H_3\mathbf{1}(O)]^{2-}$ and $[Mn^{III}H_3\mathbf{1}(O)]^{2-}$ complexes react with a variety of external species, with chemistry occurring at the oxo ligand. For instance, $[Fe^{III}H_3\mathbf{1}(O)]^{2-}$ reacts with protons and MeI to produce the corresponding $[Fe^{III}H_3\mathbf{1}(OH)]^{-}$ and $[Fe^{III}H_3\mathbf{1}(OCH_3)]^{-}$ complexes.[19c] However, transfer of the oxo ligand to external species has not been observed. We attribute this inability to transfer atoms to the placement of the M^{III}−O(H) units within a relatively constrained H-bond cavity. Modulation of the H-bond network within the cavity may alter the reactivity of the M−O(H) units and promote atom transfer.

Acknowledgment. Acknowledgment is made to the NIH (GM50781 to A.S.B. and GM49970 to M.P.H.). We are grateful to B. S. Hammes, Z. Shirin, M. Zart, P. Larsen, and M. Miller for helpful discussions.

Supporting Information Available: Crystallographic details for $K[Fe^{III}H_3\mathbf{1}(OH)]\cdot 0.5CH_3CN$ (CIF). This material is available free of charge via the Internet at http://pubs.acs.org.

JA0305151

(50) The σ-antibond molecular orbital for $[Fe^{III}H_3\mathbf{1}(O)]^{2-}$ is 77.7% dz^2(Fe) + 22.3% pz(O), and for $[Mn^{III}H_3\mathbf{1}(O)]^{2-}$ it is 9.8% s(Mn) + 66.9% dz^2(Mn) + 3.1%s(O) + 19.7% pz(O).

(51) For $[Fe^{III}H_3\mathbf{1}(O)]^{2-}$, the relative charges are +1.56 (Fe) and −1.16 (O), while for $[Mn^{III}H_3\mathbf{1}(O)]^{2-}$ they are +1.74 (Mn) and −1.16 (O).

(52) Bordwell, F. G.; Harrelson, J. A., Jr.; Zhang, X. *J. Org. Chem.* **1991**, *56*, 4448−4450.

(53) For a discussion on single versus double bonds in zirconium−oxo complexes, see: Howard, W. A.; Parkin, G. *J. Am. Chem. Soc.* **1994**, *116*, 606−615.

(54) (a) Vance, C. K.; Miller, A.-F. *Biochemistry* **2001**, *40*, 13079-13087. (b) Edward, R. A.; Whittaker, M. M.; Whittaker, J. M.; Baker, E. N.; Jameson, G. B. *Biochemistry* **2001**, *40*, 15−27. (c) Yikilmaz, E.; Xie, J.; Brunold, T. C.; Miller, A.-F. *J. Am. Chem. Soc.* **2002**, *124*, 3482−3483. (d) Xie, J.; Yikilmaz, E.; Miller, A.-F.; Brunold, T. C. *J. Am. Chem. Soc.* **2002**, *124*, 3769−3774. (e) Lah, M. S.; Dixon, M. M.; Pattridge, K. A.; Stallings, W. C.; Fee, J. A.; Ludwig, M. L. *Biochemistry* **1995**, *34*, 1646−1660.

(55) (a) Dawson, J. H. *Science* **1988**, *240*, 433−439. (b) Martinis, S. A.; Atkins, W. M.; Stayton, P. S.; Sligar, S. G. *J. Am. Chem. Soc.* **1989**, *111*, 9252−9253. (c) Gerber, N. C.; Sligar, S. G. *J. Am. Chem. Soc.* **1992**, *114*, 8742−8743. (d) Ozaki, S.; Roach, M. P.; Matsui, T.; Watanabe, Y. *Acc. Chem. Res.* **2001**, *34*, 818−825.